ESEEM Investigations of the High pH and Low pH Forms of Chicken Liver Sulfite Oxidase

Arnold M. Raitsimring,* Andrew Pacheco,* and John H. Enemark*

Contribution from the Department of Chemistry, University of Arizona, Tucson, Arizona 85721

Received June 1, 1998

Abstract: Two-pulse and four-pulse electron spin−echo envelope modulation spectroscopy (ESEEMS) at two operational frequencies and two-dimensional hyperfine sublevel correlation spectroscopy (HYSCORES), have been used to probe the Mo^V coordination environment of sulfite oxidase in H_2O and D_2O solutions, buffered at pH 9.5 and 7.0 with ∼100 mM Tris-type buffers. At pH 9.5 the ESEEM and HYSCORE results definitively reveal the presence of one solvent-exchangeable D(H) near the Mo^V center, probably in the form of a Mo−OH(D) moiety. The orientation of this group is not fixed (although it is substantially restricted) and thus gives rise to a distribution of hyperfine interaction (*hfi*) parameters. The resulting loss of amplitude makes direct observation of a proton-related line using ESEEM impossible. However, such a line is observable in ESEEM spectra of the comparable deuterated enzyme because the narrower distribution of *hfi* parameters leads to less line broadening of the ESEEM spectra. ESEEM and HYSCORE spectra of sulfite oxidase obtained at pH 7.0 show no evidence of nearby H(D) groups, other than the single exchangeable proton/deuteron readily detected by CW EPR spectroscopy, which is also believed to be part of a Mo−OH(D) moiety. The differences observed in the Mo···H(D) *hfi* parameters of SO as the pH is varied probably result from relatively small displacements of the H(D), which move the nucleon in and out of a node of the singly occupied Mo d orbital.

Introduction

Mo and W are the only second and third row transition metals that have a known biological function. Mo is associated with more than thirty enzymes that catalyze key 2-electron oxidation−reduction reactions in the metabolism of C, N, and S by microorganisms, plants, and animals by a formal oxygen atom transfer process[1]

$$X + H_2O \rightleftharpoons XO + 2H^+ + 2e^-$$

Prior to 1995 no mononuclear Mo or W enzymes had been crystallographically characterized; however, since then, seven structure determinations have been reported.[2−8] These structures have shown that the active sites have a single Mo atom coordinated by the ene-1,2-dithiolate group of one or two novel pyranopterin ligands (often referred to as "molybdopterins", Structure **1**). With the availability of these crystal structures, the investigation of molybdoenzymes has entered a new phase, in which more detailed questions about enzyme structure and function can be addressed. In particular in our laboratories we

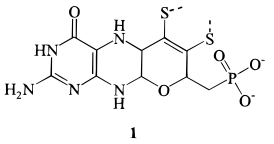

1

are using powerful spectroscopic and kinetic methods to investigate transient states of sulfite oxidase that may play a key role in the overall catalytic cycle.

Sulfite oxidase catalyzes the oxidation of sulfite to sulfate, coupled with the subsequent reduction of 2 equiv of ferricytochrome *c* (cyt *c*)$_{ox}$ to ferrocytochrome *c* (cyt *c*)$_{red}$[1]

$$SO_3^{2-} + H_2O + 2(\text{cyt } c)_{ox} \rightleftharpoons SO_4^{2-} + 2(\text{cyt } c)_{red} + 2H^+$$

This is the terminal reaction in the oxidative degradation of sulfur-containing compounds and is physiologically essential. Chicken liver sulfite oxidase (SO) is typical of the enzyme in higher vertebrates and consists of two identical subunits, each with a molecular weight of ∼51.5 kDa.[9] Each subunit in turn has two functionally distinct domains. The smaller N-terminal domain (∼10 kDa) contains a b_5-type heme center; in the resting enzyme, the Fe is in oxidation state III. The larger C-terminal domain (∼42 kDa) contains a Mo atom with a resting oxidation state of VI. The two-electron oxidation of SO_3^{2-} occurs at the Mo center to give formally Mo^{IV}, which is then reoxidized to Mo^{VI} by sequential one-electron transfers to the b_5-type heme center. After each Mo → Fe one-electron-transfer step, the b_5 center is reoxidized by exogenous (cyt *c*)$_{ox}$, thus completing the turnover process.[1,10]

If a sample of SO is reduced in the absence of cyt *c* and immediately frozen in liquid N_2, then characteristic Mo^V EPR

(1) Hille, R. *Chem. Rev.* **1996**, *96*, 2757−2816.
(2) Chan, M. K.; Mukund, S.; Kletzin, A.; Adams, M. W. W.; Rees, D. C. *Science* **1995**, *267*, 1463−1469.
(3) Romao, M. J.; Archer, M.; Moura, I.; Moura, J. J. G.; LeGall, J.; Engh, R.; Schneider, M.; Hof, P.; Huber, R. *Science* **1995**, *270*, 1170−1176.
(4) Schindelin, H.; Kisker, C.; Hilton, J.; Rajagopalan, K. V.; Rees, D. C. *Science* **1996**, *272*, 1615−1621.
(5) Schneider F.; Lowe J.; Huber R. H. S.; Kisker, C.; Knablien, J. *J. Mol. Biol.* **1996**, *263*, 53−59.
(6) Boyington, J. C.; Gladyshev, V. N.; Khangulov, S. V.; Stadtman, T. C.; Sun, P. D. *Science* **1997**, *275*, 1305−1308.
(7) Kisker, C.; Schindelin, H.; Pacheco, A.; Wehbi, W.; Garret, R. M.; Rajagopalan, K. V.; Enemark, J. H.; Rees, D. C. *Cell* **1997**, *91*, 973−983.
(8) McAlpine, A. S.; McEwan, A. G.; Shaw, A. L.; Bailey, S. *J. Biol. Inorg. Chem.* **1997**, *2*, 690−701.
(9) Sullivan, E. P., Jr.; Hazzard, J. T.; Tollin, G.; Enemark, J. H. *Biochemistry* **1993**, *32*, 12465−12470.
(10) Pacheco, A.; Hazzard, J. T.; Tollin, G.; Enemark, J. H., submitted.

10.1021/ja981903j CCC: $15.00
Published on Web 10/21/1998

signals are obtained.[11−14] Extensive CW EPR investigations of sulfite oxidase (SO) during the late 1970s and early 1980s, carried out primarily by Bray and co-workers, demonstrated that SO exhibits three EPR distinct forms.[11−14] In high pH buffers (pH 9−9.5) containing low anion concentrations, one form is obtained exclusively, whereas the other two are observed in buffers of ∼pH 7 containing high concentrations of anions such as Cl^- or phosphate. At intermediate pH values, mixtures of species are observed. Which of the low pH forms is observed depends on whether phosphate is present in the buffer, and thus, these two forms have become known as the low 'pH form' (*lpH*) and the 'phosphate inhibited form' (*Pi*). Similarly, the species observable at high pH has become known as the 'high pH' (*hpH*) form.

The *lpH* form clearly shows well resolved doublets at the g_z and g_x positions, which disappear in D_2O buffer. This finding allowed Bray and co-workers[12] to conclude that the observed splitting is caused by hyperfine interaction (*hfi*) of Mo^V with a single strongly coupled (SC) exchangeable proton, most probably belonging to a Mo−OH group. From numerical simulations of the CW spectrum Bray and co-workers obtained the *hfi* tensor associated with the SC proton;[12] however, low resolution precluded obtaining such important structural information as the relative orientations of the Mo−O−H atoms.

The above-mentioned proton splitting is not observed for either the *Pi* or *hpH* forms of the enzyme. In the case of the *Pi* form, CW EPR experiments using partially ^{17}O-substituted PO_4^{2-} provided early evidence that a phosphate group coordinates to the Mo^V center, displacing OH^-;[13] this suggestion was recently confirmed by ESEEM spectroscopy.[15] Recent CW EPR and Mo K edge EXAFS studies of SO in the presence of arsenate at pH 6.5 reveal Mo···As interactions consistent with the formation of the analogous monodentate arsenate complex.[16] For the *hpH* form, the lack of an exchangeable proton was initially believed to reflect deprotonation of the putative Mo−OH group in the *lpH* form. Later however, George proposed that a Mo−OH moiety was also present at high pH.[17] This suggestion was supported by earlier ^{17}O studies which showed that, unlike the *Pi* form, both the *hpH* and *lpH* forms have one water-exchangeable oxygen-containing ligand.[11] An OH moiety would be a likely candidate for this ligand, and George[17] suggested a possible mechanism involving pH-dependent coordination changes that might explain the transition from the *lpH* to the *hpH* form without invoking loss of Mo−OH.

At this stage, having reached the limitations imposed by the innate low resolution of CW EPR, investigations relating to the structural nature of the EPR-active species of SO stagnated and have remained unresolved for a decade. However, during this time electron spin−echo envelope modulation spectroscopy (ESEEM) has undergone substantial growth, with significant advances in theoretical understanding, and the development of new pulse sequences, techniques of multiband operation, and methods for simulating ESEEM spectra computationally. All of these advances have contributed to making ESEEM a very effective tool for investigating structural problems. In particular, as was recently demonstrated by Dikanov[18] and McCracken,[19] the investigation of OH_2 or OH groups coordinated to metal ions seems to be a problem tailor-made for ESEEM. Protons of coordinated OH_2 or OH groups are situated at a favorable 2.5−3 Å from the metal center, and M−H interactions result in reasonably intense spectral features known as "sum-combination" lines, which are cleanly separated from all other spectral features. Analyzing the dependence of peak intensity and position of the sum-combination lines on the magnetic field across the CW EPR spectrum yields the desired structural information.

Herein we report a detailed investigation of the *lpH* and *hpH* forms of SO, which made use of two-pulse and four-pulse ESEEM at two operational frequencies and the technique of two-dimensional hyperfine sublevel correlation spectroscopy (HYSCORES).[20] The results of this investigation have become particularly relevant in the wake of the crystal structure determination of SO, obtained after the ESEEM investigation was well under way,[7] which among other things has raised anew the questions about the nature of the *hpH* and *lpH* forms. Structure **2** schematically summarizes the coordination geometry

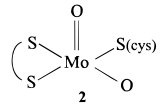

2

of the Mo center of SO, revealed by the crystal structure.[7] The geometry is approximately square pyramidal, with an oxo group occupying the apical position. The equatorial positions are occupied by a second oxygen and by three sulfurs; one sulfur is supplied by a cysteine side chain, while the other two come from the ene-dithiolate group of the molybdopterin (cf. Structure **1**). The crystal structure reveals that the equatorial oxygen ligand is accessible to the solvent, whereas the apical one is not;[7] this fact, together with recent resonance Raman and ^{18}O-labeling experiments,[21] suggests that the equatorial oxygen atom is transferred during catalysis and is the one protonated in the Mo^V form of the enzyme. A putative sixth coordination site at the Mo center is effectively blocked by the protein backbone. This raises a problem because every explanation for the difference between the *hpH* and *lpH* forms of SO which had been suggested prior to the structure determination had invoked Mo coordination of a Cl^- in the *lpH* form.[14,22] Such proposals explained the observation that the equilibrium between the *hpH* and *lpH* forms of the enzyme can be shifted at constant pH toward the *lpH* form by addition of Cl^-;[14,22] however, the crystal structure does not reveal any obvious site at which Cl^- could bind. The kinetic investigations described in our related paper[10] and the detailed spectroscopic characterization of the *hpH* and *lpH* forms of SO described in this article reveal a possible explanation for the *lpH*/*hpH* equilibrium which does not invoke anion binding to the Mo center. This explanation also provides insight into the mechanism of intramolecular electron transfer between the Mo and Fe centers of SO.[10]

Theory

We will consider two kinds of spin systems, consisting of either a proton ($I = {}^1/_2$) or a deuteron ($I = 1$), and a Mo^V ($S =$

(11) Cramer, S. P.; Johnson, J. L.; Rajagopalan, K. V.; Sorrell, T. S. *Biochem. Biophys. Res. Commun.* **1979**, *91*, 434−439.
(12) Lamy, M. T.; Gutteridge, S.; Bray, R. C. *Biochem. J.* **1980**, *185*, 397−403.
(13) Gutteridge, S.; Lamy, M. T.; Bray, R. C. *Biochem. J.* **1980**, *191*, 285−288.
(14) Bray, R. C.; Gutteridge, S.; Lamy, M. T.; Wilkinson, T. *Biochem. J.* **1983**, *211*, 227−236.
(15) Pacheco, A.; Basu, P.; Borbat, P.; Raitsimring, A. M.; Enemark, J. H. *Inorg. Chem.* **1996**, *35*, 7001−7008.
(16) George, G. N.; Garrett, R. M.; Graf, T.; Prince, R. C.; Rajagopalan, K. V. *J. Am. Chem. Soc.* **1998**, *120*, 4522−4523.
(17) George, G. N. *J. Magn. Reson.* **1985**, *64*, 384−394.
(18) Tyryshkin, A. M.; Dikanov, S. A.; Goldfarb, D. *J. Magn. Reson.* **1993**, *A105*, 271−283.
(19) McCracken, J.; Friedenberg, S. *J. Phys. Chem.* **1994**, *98*, 467−473.
(20) Höfer, P.; Grupp, A.; Nebenführ, H.; Mehring, M. *Chem. Phys. Lett.* **1986**, *132*, 279−282.
(21) Garton, S. D.; Garrett, R. M.; Rajagopalan, K. V.; Johnson, M. K. *J. Am. Chem. Soc.* **1997**, *119*, 2590−2591.
(22) Bray, R. C. *Polyhedron* **1986**, *5*, 591−595.

$^1/_2$). The spin-Hamiltonian in the first case is

$$H = \beta_e \vec{S}^T \mathbf{g} \vec{B}_m - g_n \beta_n \vec{I}^T \vec{B}_m + \vec{I}^T \mathbf{D} \vec{S} \qquad (1)$$

where the terms represent the electron Zeeman, the nuclear Zeeman and the *hfi*, respectively. **D** in turn can be split into $\mathbf{D} = a_0\mathbf{E} + \mathbf{T}$, where ($a_0\mathbf{E}$) is the isotropic and (**T**) the anisotropic part of the *hfi* (**E** is a unity matrix). A *hfi* results in two fundamental frequencies, ν_α and ν_β, which in the **g** tensor reference coordinate frame (RCF) are[23]

$$\nu_{m_s} = |\vec{h}^{\pm}|;\ \vec{h}^{\pm} = [(m_s A_1 - \nu_I l_1),\quad (m_s A_2 - \nu_I l_2),\quad (m_s A_3 - \nu_I l_3)] \qquad (2)$$

Here l_i are the directional cosines of the external magnetic field $\mathbf{B}_m$ in the RCF, and $m_s = \pm^1/_2$ for the α and β manifolds of electron spin, respectively. An expression for A_i applicable to an arbitrary **D** may be found elsewhere;[24] for the particular case of axial anisotropic interaction, which assumes that $\mathbf{T} \equiv (-T, -T, 2T)$ in its own principal axis, and when there is small absolute variation of the principal *g* values, the A_i may be written in the following way:

$$A_i = T[l_i((3n_i^2 - 1) + a_0/T) + 3n_i \sum_{k \neq i} l_k n_k] \qquad (3)$$

where n_i are the directional cosines of $\mathbf{z}_h$, the *z* principal axis of the anisotropic *hfi* tensor in the RCF. In the point dipolar approximation (PDA) both *T* and $\mathbf{z}_h$ have certain physical meanings: $\mathbf{z}_h$ is the unit vector of the radius-vector **r** which connects the electron and nuclear spins, while $T = g_e\beta_e\beta_n g_n/\hbar r^3$ (g_e is the average electronic *g* value).

In primary spin−echo the *hfi* manifests itself as a modulation of the ESE signal with two fundamental (*f*), $\omega_{\alpha(\beta)} \equiv 2\pi\nu_{\alpha(\beta)}$, and two combination frequencies, sum (*s*) and difference (*d*), $\omega_\pm = \omega_\alpha \pm \omega_\beta$, such that the modulation pattern is given by

$$V(\tau) \propto 1 - \frac{k}{2} + \frac{k}{2}[\cos(\omega_\alpha\tau) + \cos(\omega_\beta\tau)] - \frac{k}{4}[\cos(\omega_+\tau) + \cos(\omega_-\tau)] \qquad (4)$$

Here the intensity parameter, *k*, is[25]

$$k = \left(\frac{\nu_I}{\nu_\alpha\nu_\alpha}\right)^2 [(A_1l_2 - A_2l_1)^2 + (A_2l_3 - A_3l_2)^2 + (A_1l_3 - A_3l_1)^2] \qquad (5)$$

The ESEEM spectrum, which is the Fourier transform (FT) of the time domain, correspondingly consists of two *f*- and two combination (*s*- and *d*-) lines, with intensities *k/2* and *k/4*, respectively. The behavior of these lines for various relations between nuclear Zeeman and hyperfine interactions has been thoroughly investigated and described.[26] For further practical applications, the most interesting of all of these lines is the *s*-line, which in the case of a weak *hfi*, i.e., $\omega_I \gg A_i/2$, is substantially less broadened by anisotropic *hfi* than all the others, and usually appears in ESEEM spectra as a single peak with a well-defined maximum, even for orientationally disordered systems. The maximum of this line also has a characteristic shift δ' from the double Larmor nuclear frequency, $\delta' = \omega_+ - 2\omega_I$, which is directly related to the anisotropic *hfi*.[27,28] For instance, for one of the canonical orientations, say $l_3 = 1$

$$\delta' \simeq \left(\frac{3}{2}T \sin\theta_n \cos\theta_n\right)^2/\omega_I \qquad (6)$$

where θ_n is an angle which $\mathbf{z}_h$ makes with the *z* axis of the RCF.

A nuclear quadrupole interaction *(nqi)* adds to the spin-Hamiltonian the term $I^T\mathbf{Q}I$, where **Q** is the nuclear quadrupole coupling tensor (*NQCT*). In general, the interaction of an electron spin with quadrupolar nuclei results in ESEEM spectra which are quite complicated and whose interpretation requires massive multiparametric simulations.[26,29] However, interpretation becomes unambiguous and straightforward in a weak quadrupole interaction limit, i.e., if *nqi* can be considered as a perturbation to the nuclear Zeeman interaction, +*hfi*. A small magnitude for the nuclear quadrupole coupling constant, q_0 (e.g., 0.2−0.25 MHz for D in D_2O[30]) does not automatically provide this limit, but it may be reached by corresponding adjustment of the operational frequency. As will be discussed in the Experimental Section, the operational frequency in these experiments was always chosen so that *nqi* was weak.

A weak quadrupole interaction splits each fundamental frequency, determined by eq 2, into two[31,32]

$$\nu_{\alpha,\beta}{}^{\pm} = \nu_{\alpha,\beta} \pm \Delta_{\alpha,\beta};\quad \nu_{\alpha,\beta} \gg \Delta_{\alpha,\beta} \qquad (7)$$

and these splittings were calculated in the manner derived by Toriyama and Iwasaki[33] (see also ref 29).

It has been shown[34] that a weak quadrupole interaction causes only minor alteration of the transition probability, and therefore, parameter *k*, determined by eq 5, may still be used for evaluation of the modulation amplitude. Modulation of the primary spin−echo for $S = ^1/_2$ and $I = 1$ has been derived and may be written as[31,32]

$$V(\tau) \propto 1 - 4\frac{k}{3} + 2\frac{k}{3}[\cos(\omega_\alpha{}^+\tau) + \cos(\omega_\beta{}^+\tau) + \cos(\omega_\alpha{}^-\tau) + \cos(\omega_\beta{}^-\tau)] - 2\frac{k}{3}[\cos(\omega_\alpha{}^+\tau)\cos(\omega_\beta{}^+\tau) + \cos(\omega_\alpha{}^-\tau)\cos(\omega_\beta{}^-\tau)] \qquad (8)$$

neglecting higher orders of *k*. As one can see from eqs 7 and 8, the splitting caused by *nqi* in the *s*-line is double that observed in the *f*-lines. Since the *s*-line is also substantially less broadened than the *f*-lines by anisotropic *hfi*, it is obvious that measurements of *nqi* parameters have to be performed utilizing the *s*-line. In principle, the two-pulse technique can be used

(23) (a) Hoffman, B. M.; Martinsen, J.; Venters, R. A. *J. Magn. Reson.* **1984**, *59*, 110−123. (b) Hurst, G. C.; Henderson, T. A.; Kreilick, R. W. *J. Am. Chem. Soc.* **1985**, *107*, 7294−7299.

(24) Dikanov, S. A.; Xun, L.; Karpiel, A. B.; Tyryshkin, A. M.; Bowman, M. K. *J. Am. Chem. Soc.* **1996**, *118*, 8408−8416.

(25) Raitsimring A. M.; Borbat, P.; Shokhireva, T.; Walker, F. A. *J. Phys. Chem.* **1996**, *100*, 5235−5244.

(26) Dikanov, S. A.; Tsvetkov, Yu. D. *Electron Spin-Echo Modulation (ESEEM) Spectroscopy*; CRC Press: Boca Raton, FL, 1992; Chapter 6.

(27) Reijerse, E.; Dikanov, S. *J. Chem. Phys.* **1991**, *95*, 836−845.

(28) Schweiger, A. In *Advanced EPR Applications in Biology and Biochemistry*; Hoff, A. J., Ed.; Elsevier: 1989; pp 243−275.

(29) Tyrishkin, A. M.; Dikanov, S. A.; Reijerse, E. J. *J. Magn. Reson.* **1995**, *A116*, 10−21.

(30) Weiss, A.; Weiden, N. In *Advances in Nuclear Quadrupole Resonance*; Smith, J. A. S., Ed.; Heyden and Son Ltd: Cambridge, 1980; Vol. 4, pp 149−269.

(31) (a) Mims W. B. *Phys. Rev. B: Solid State* **1972**, *5*, 2409−2419. (b) Mims, W. B. *Phys. Rev. B: Solid State* **1972**, *6*, 3543−3545.

(32) Shubin A. A.; Dikanov, S. A. *J. Magn. Reson.* **1985**, *64*, 185−193.

(33) Iwasaki M.; Toriyama, K. In *Electron Magnetic Resonance of the Solid State*; Weil, J. A., Bowman, M. K., Morton, J. R., Preston, K. F., Eds; The Canadian Society of Chemistry: Ottawa, ON, Canada, 1987; pp 545−570.

(34) Ichikawa, T. *J. Chem. Phys.* **1985**, *83*, 3790−3797.

for such measurements. However, the applicability of this technique to a particular experiment depends on phase memory time, which may severely limit the time interval available for measurements, and cause a loss of resolution in the subsequent FT. These complications can be reduced by applying a four-pulse technique which also generates *s*-lines. The four-pulse technique has the drawback of substantial loss of the signal amplitude but does increase the available time interval and, subsequently, resolution in the frequency domain. An analytical expression for four-pulse ESEEM in the presence of a weak quadrupole interaction has been derived by Dikanov and co-workers.[18] The entire expression is too cumbersome to be presented here; only the part necessary for further discussion of the *s*-line when $k \ll 1$ is extracted and presented as eq 9.

$$V(\tau/2,t/2) \propto k\left\{\sin\frac{\omega_\alpha^{+}\tau}{2}\sin\frac{\omega_\beta^{+}\tau}{2}\cos\frac{(\omega_\alpha^{+}+\omega_\beta^{+})(\tau+t)}{2} + \sin\frac{\omega_\alpha^{-}\tau}{2}\sin\frac{\omega_\beta^{-}\tau}{2}\cos\frac{(\omega_\alpha^{-}+\omega_\beta^{-})(\tau+t)}{2}\right\} \quad (9)$$

Comparing eq 9 with the expression for two-pulse ESEEM (eq 8), one may note that in the four-pulse method the amplitude of the *s*-line contains additional factors that depend on the time interval between the first and second pulse, τ. This feature is used to suppress undesired modulation patterns. For the sake of further application, we would also mention that if the *hfi* is weak, then the fundamental frequencies merge, $\nu_\alpha \approx \nu_\beta \approx \nu_I$ and the quadrupole splittings for both manifolds are equal, $\Delta_\alpha \approx \Delta_\beta$. For canonical orientations (e.g., $l_3 = 1$), if the asymmetry parameter is neglected (as is common practice for deuterons), then the *s*-line is split[35] by

$$\delta = \frac{3}{2}q_0(1 - 3\cos^2\psi) \quad (10)$$

where ψ is the angle between the principal axis ($\mathbf{z}_q$) of the *NQCT*, and the corresponding *Z*-axis of the RCF. Interaction of nuclei randomly oriented around the paramagnetic center results in an *s*-line that consists of two peaks and shoulders with splittings $\delta = {}^3/_2 q_0$ and 2δ (see, for example, ref 38). Only the peaks are observable in the ESEEM spectra due to the statistical weight factor, and thus the shape of an *s*-line is a doublet. The q_0 related to the observed doublet splitting is $q_0 = 2\delta/3$.

If the ESEEM spectrum results from interaction with more than one nucleon *(i)*, then the time domain pattern for both the two-[31] and four-[18] pulse methods is

$$V(\tau) = \prod V^{(i)}(\tau); \quad V(\tau,t/2) = \prod V^{(i)}(\tau,t/2) \quad (11)$$

In a disordered (or partly oriented) system a given field, B_m does not represent a unique orientation, but rather a set of orientations and, consequently, a set of frequencies. Therefore, to calculate the ESEEM pattern, eq 11 must be averaged over all of the orientations available at the given B_m and then averaged again over a distribution of the resonant fields in accord with an individual line shape and pulse width. Numerical simulations of the ESEEM spectra were performed in the following manner. For averaging over space, a uniform grid for $\cos\theta$ and ϕ of 1000×500 points was used. The orientation was accepted if $|h\nu_0 - \beta_e g_e B_m| \le \beta_e g_e B_1/2$, where B_1 is the pulse amplitude and g_e is effective *g* value

$$g_e = \sum_i \sqrt{(g_i l_i)^2} \quad (12)$$

The individual line width and shape was taken as $\exp\{-((B - B_m)/\chi)^2)\}$. The averaging over *B* was performed within the limits $\pm 2\chi$, with steps of 0.1χ. The time steps in the simulations were chosen to be the same as in the respective experiments. The time domain pattern calculated in this way was then subjected to the same FT procedure that was used in the experiment, with the experimental values of the dead time and time interval.

Experimental Section

Highly pure samples of SO in the appropriate D_2O and H_2O buffers were prepared as previously described.[15] The *lpH* and *hpH* forms were obtained in buffers containing 100 mM Tris, 6.3 mM Tris HCl, 100 mM NaCl (pH = 7.0, *lpH*), and 100 mM bis Tris propane, 26.9 mM Tris HCl (pH = 9.55, *hpH*), respectively. The *Pi* form was obtained as previously described.[15] The final Mo^V concentration in all samples was approximately 0.6 mM. CW EPR spectra were recorded at 77 K on a ESP-300E Bruker X-band spectrometer. The observed *g* values and splittings (for the *lpH* form) were in good agreement with those previously reported.[12] Two-pulse, four-pulse, and HYSCORE measurements were performed using a home-built multifrequency pulsed EPR spectrometer,[36] on deuterated and protonated samples, at operational frequencies of 15.2−15.4 GHz and 8.7−8.9 GHz. Recording conditions were generally as follows: temperature, 20−25 K; repetition rate, 200−300 Hz; typical acquisition time, 15−30 min for a one-dimensional experiment. Typical conditions for two-pulse ESE were $2\pi/3-2\pi/3$ pulses with a pulse duration of 17−20 ns, providing pulse amplitudes of 16−20 MHz; dead time, 240−320 ns; τ increment of 5−10 ns. The available time interval was limited to 1500−2000 ns because of short phase-memory time ($0.6\ \mu s^{-1}$). Four-pulse and HYSCORE experiments used the pulse sequence $\pi/2-\tau-\pi/2-t/2-\pi-t/2-\pi/2$; the $\pi/2$ pulse duration was 30 ns; for the π-pulse, a second independent mw-channel was used, and the duration of this pulse was 15−17 ns; *t*/2 increment (unless otherwise specified) was 20−25 ns; time interval, 6.0−7.5 μs; interval τ between the first and second pulses was varied between 220 and 400 ns. To eliminate unwanted transients, a common phase cycle was applied.[37] The HYSCORE experiments used the same pulse durations and amplitudes as the four-pulse technique, with 25 ns steps in the t_1-t_2 directions. Generally, 200−250 points were collected in each direction, which required about 3−4 h acquisition time. All one-dimensional spin−echo measurements were performed through the entire CW EPR spectrum in steps of 5−10 G, which corresponds to about twenty acquisitions per sample.

In accord with the theoretical analysis presented in the previous section, the operational frequency for investigation of deuterated samples was chosen such that *nqi* and *hfi* were in the weak interaction limit, yet a reasonable modulation amplitude could still be achieved. This greatly facilitated data analysis and interpretation. After evaluating the preliminary experiments and published data,[12] a ν_0 of 15−15.5 GHz was found to provide a good compromise between the aforementioned requirements.

For measurements on protonated samples, the requirements for optimizing the instrumental setup are rather complex; only two are mentioned here. Quantitative measurements of line amplitudes may be performed only in the case of full excitation of hyperfine transitions, i.e., when pulse amplitudes exceed the corresponding *f*-frequencies. On the other hand, pulse amplitudes of more than the natural EPR line width result in a loss of orientational resolution and, subsequently, absolute intensity of the *f* and *s* lines in the ESEEM spectra. By taking into account these facts and the fact that the CW line width found in *X*-band is 15−20 MHz,[12] pulse amplitudes of 20 MHz and the lowest

(35) Tyryshkin, A. M.; Dikanov, S. A.; Evelo, R. G.; Hoff, A. J. *J. Chem. Phys.* **1992**, *97*, 42−49.

(36) Borbat, P.; Raitsimring, A. M. *A new pulse EPR spectrometer at the University of Arizona*, Abstracts of the 36th Rocky Mountain Conference on Analytical Chemistry, Denver, CO, July 31−August 5, 1994; p 94.

(37) Gemperle, C.; Aebli, G.; Schweiger, A.; Ernst, R. R. *J. Magn. Reson.* **1990**, *88*, 241−256.

available operational frequency (8.6−8.7 GHz) were used in order to decrease the nuclear Larmor proton and *f*-frequencies correspondingly. Under these conditions, modulation from the SC proton in the *lpH* form has to be substantially suppressed, because one of its *f*-frequencies is reached at ∼30 MHz, which exceeds the pulse amplitude. Still, such suppression might facilitate the observation of interaction with a second nearby proton (vide infra).

Results and Discussion

Phosphate Inhibited Form of SO in D_2O. The modulation of the spin−echo signal in the *lpH* and *hpH* forms of SO results not only from directly coordinated ligands but also from distant nuclei which belong to noncoordinated water molecules and neighboring amino acid residues. Removing such background or matrix modulation from the overall modulation pattern, particularly for samples in D_2O, is not a trivial problem because of strong overlap between the desired and unwanted lines. This difficulty is exacerbated by the decreased *hfi* interaction for deuterons compared to protons. In the past, depending on the features of the particular system under investigation, this overlap problem has been solved in a variety of ways. For instance, rejection filtration on the experimental spectrum at the Larmor deuterium frequency has been used to eliminate matrix modulation.[38] Others have assumed models for the distribution of distant nuclei to perform the simulations of background modulation and consequently to eliminate it from the experimental pattern.[18] In the present case, we have taken the background modulation directly from experimental data collected for the *Pi* form of SO, in which a phosphate group coordinates directly to Mo at the position otherwise occupied (vide infra) by an OH-(D) group.[15] In a reasonably isotropic environment, substitution of an OH(D) group by a phosphate group should not significantly affect the environment of nuclei that are distant from the Mo^V center. However, in an anisotropic medium such as an enzyme, even distant nuclei might have some spatial or orientational preferences as a result of, for example, hydrogen bonding. Since all of the forms of SO have different principal *g* values and may have relatively differently oriented RCF, the possibility of spatial or orientational preferences in the *Pi* form had to be ruled out before applying this background modulation to the *lpH* and *hpH* forms.

Typically, nuclei are considered randomly distributed around a paramagnetic ion if modulation does not show specific orientational selectivity, i.e., if it does not depend on the magnetic field through the CW spectrum or, in other words, on orientation of the magnetic field vector in the RCF. On the basis of this reasoning, the absolute intensities of the $^2H(D)$ modulation throughout entire CW EPR spectrum of the *Pi* form were thoroughly investigated to test whether the distant D nuclei in SO are randomly distributed. Figure 1a shows a representative example of a two-pulse ESEEM spectrum, collected near the g_y field position. The lines marked as *f* and *s* result from interaction of the Mo^V electron with $^2H(D)$, ^{31}P, and ^1H nuclei. The deuteron Larmor (*f*) and double Larmor (*s*) frequencies for the $^2H(D)$ lines depend on the applied magnetic field ($\mathbf{B}_m$), and their position and shape are typical for the interaction of an electron spin with distant nuclei (Figure 1). The normalized intensities of the fundamental (*f*) and sum combinational (*s*) lines (5.6 ± 0.2 and 1.4 ± 0.2%, respectively) are constant within the limits of experimental accuracy across the CW EPR spectrum (see Supporting Information), providing the first confirmation of random nuclear distribution. The 4:1 ratio of *f*- to *s*-line intensities is also a well-known feature of the interaction with distant protons or deuterons, i.e., nuclei with extremely weak *hfi* (see Theory, eq 4 or ref 26 p 92).

A second proof of the random distribution of distant deuterons came from the investigation of the quadrupole splittings. Because only a limited time interval (2000 ns) is available in a two-pulse experiment, neither the *f*- nor *s*-lines show quadrupole splitting. To observe this splitting and to examine its variation across the EPR spectrum, a four-pulse experiment was performed. Figure 1b presents two four-pulse ESEEM time-domain patterns, collected at approximately the g_y field position, using $\tau = 240$ and 340 ns, respectively; a set of experiments performed at various τ demonstrated that the maximum intensity of the *s*-line is observed at $\tau = 330-350$ ns. FT of these time domains (Figure 1c) yields spectra similar to those of Figure 1a, although intensities differ because of the τ-dependence. Note, however, that the D *s*-line, enlarged in the insert of Figure 1c, now shows a resolved quadrupole splitting. This quadrupole splitting (δ) was found to be equal to 0.34 ± 0.02 MHz, and within the limits of experimental accuracy, the magnitude was independent of magnetic field. The q_0 derived from this value ($q_0 = 2\delta/3$, see Theory) is 0.21−0.24 MHz, which is within the range of quadrupole coupling magnitudes for water molecules or OD groups in various environments, previously determined using NQR experiments.[30]

To conclude, the independence of modulation amplitude and quadrupole splitting over the entire CW EPR spectrum validates the assumption that distant nuclei do not have specific orientations, and thus the background modulation of the *Pi* form of SO may be utilized for other SO forms, despite the differences in principle *g* values.

Phosphate Inhibited Form of SO in H_2O. The ESEEM of *Pi* in H_2O was investigated at 8.9 GHz and at various magnetic field strengths across the entire EPR spectrum, to learn about the positions and absolute amplitudes of ^1H lines. A representative example of a FT two-pulse ESEEM spectra, is shown at the top of Figure 2. This spectrum shows the interaction of Mo^V with distant protons, which results in *f*- and *s*-lines situated at the proton Larmor and double Larmor frequencies. In addition, the Mo^V-P interaction gives rise to an *s*-line. The intensities of ^1H lines do not depend on the magnetic field, and the absolute magnitudes of the peak amplitudes are ∼5% (*f*-lines) and ∼3% (*s*-line), respectively. The theoretical 4:1 ratio in intensities of the *f*/*s* lines does not hold in this case (cf. the samples in D_2O) because even for distant protons (≥4 Å) the *f*-lines are subjected to dipolar broadening, effectively resulting in a decrease of *f*-line amplitude. No indication of nearby protons (<4 Å) was observed in this sample.

High-pH Form. A representative two-pulse ESEEM spectrum of *hpH* SO in H_2O is presented at the bottom of Figure 2 for a field position similar to that for the analogous *Pi* spectra shown at the top of Figure 2. It is clear that, apart from the ^{31}P *s*-line in the *Pi* spectra, there is little difference between the top and bottom spectra of Figure 2. The *hpH* spectra show neither additional ^1H lines nor an increase in the absolute intensities of the ^1H lines, when compared with *Pi* spectra. One possible explanation for the absence of *s*-lines is simply that the proposal of George[17] is incorrect and that the *hpH* form actually has no OH groups coordinated to the Mo atom. Another reason for *s*-lines not being observed as expected has been found by us;[15] this explanation parallels that for decreased amplitudes of ^1H and $^2H(D)$ *f*-lines put forth by Dikanov[38] and by Warncke and McCracken.[39] In some cases, variable orienta-

(38) Dikanov, S. A.; Astashkin, A. V.; Tsvetkov, Yu. D. *Chem. Phys. Lett.* **1988**, *144*, 251−257. (b) Dikanov, S. A.; Astashkin, A. V. In *Advanced EPR Applications in Biology and Biochemistry*, Hoff, A. G., Ed.; Elsevier: 1989; pp 59−117.

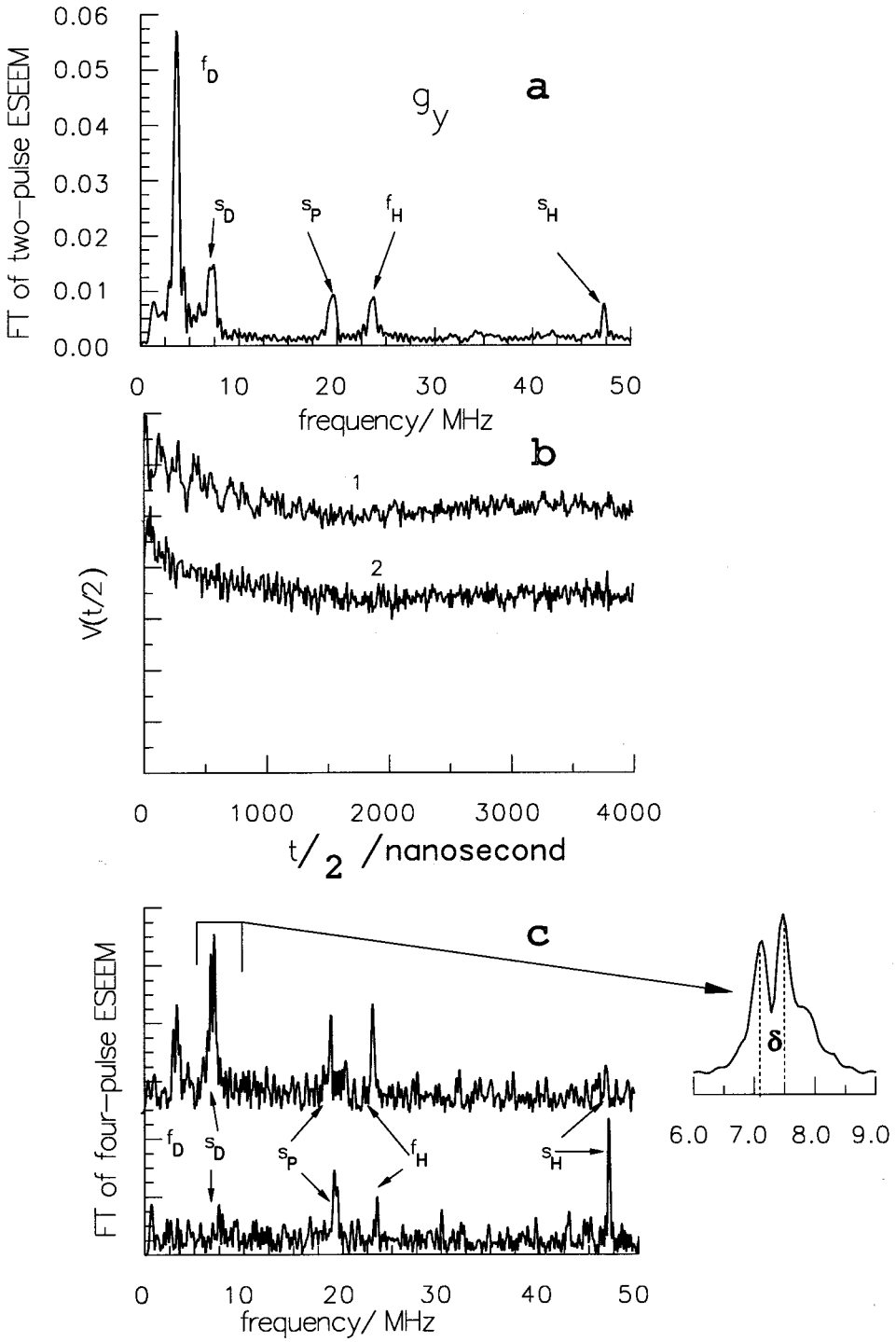

Figure 1. (a) Two-pulse normalized FT ESEEM spectra of the *Pi* form of SO in D_2O collected at an applied magnetic field of B_m (G) = 5543, which corresponds approximately to g_y for this SO form. Experimental conditions: $\nu_0 = 15.290$ GHz; pulse durations = 15ns; step of $\tau = 5$ns; time interval = 240−2240 ns; f_i and s_i denote fundamental and *s*-lines; $i \equiv {}^2$H(D), ^{31}P, and ^{1}H. (b) Time-domain four-pulse ESEEM of the *Pi* form of SO in D_2O collected at g_y. For curves 1 and 2, τ is 340 and 240 ns, respectively. $B_m = 5551$ G; $\nu_0 = 15.306$ GHz. (c) The FT of the time domain ESEEM in (b); Insert: enlargement of the D sum combinational line. For 1b $\omega_D = 3.63$ MHz.

tions of a coordinated group lead to a distribution of *hfi* parameters that can result in a severe decrease in the intensity of ESEEM spectral lines. One way to overcome this spectroscopic problem is to switch from protonated samples to deuterated ones, thereby scaling down the *hfi* 6.5 times (the ratio of gyromagnetic ratios of H and D) and therefore substantially suppressing any effects due to a possible distribution of *hfi* parameters.

Figure 3 shows the spectra of *hpH* and *Pi* samples obtained in D_2O solutions. Unlike the situation in H_2O, here direct comparison of the time domains (Figure 3a) clearly shows that the modulation is substantially deeper for the *hpH* form. This means that, in contrast with the ESEEM spectrum in H_2O, the ESEEM spectrum of the *hpH* form in D_2O directly reveals the presence of D-containing group(s) close to the metal ion. To determine the number of nearby deuterons and their distance from the Mo^V center, the modulation resulting from background

(39) Warncke, K.; McCracken, J. *J. Chem. Phys.* **1995**, *103*, 6829−6840.

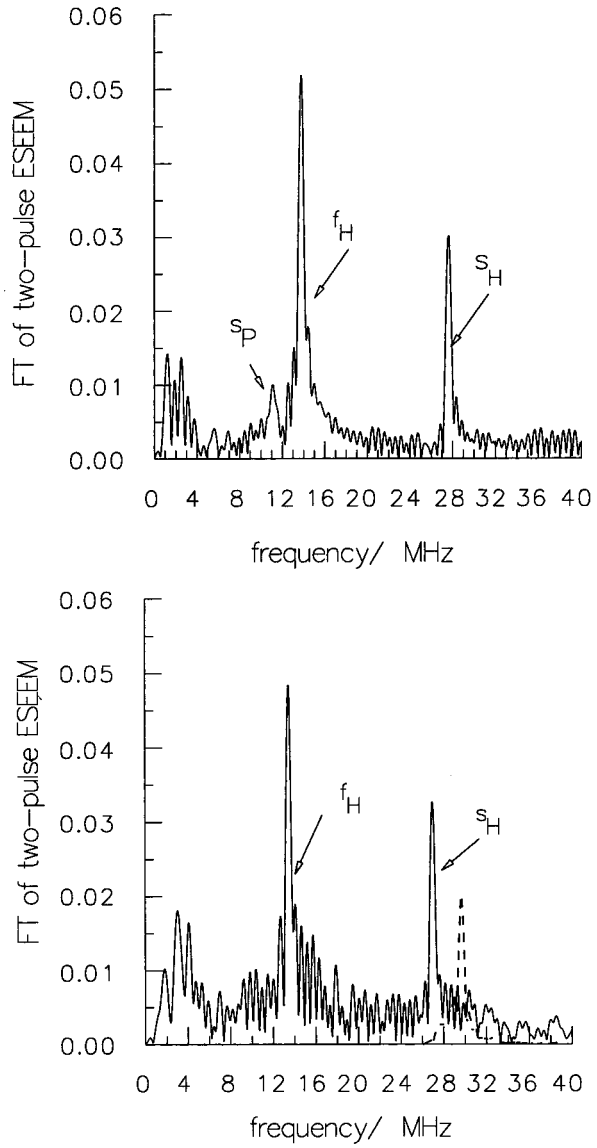

Figure 2. Normalized primary FT ESEEM spectra of the *Pi* (top) and *hpH* (bottom) forms of SO, in H_2O, at their approximate g_y position. Top: $\nu_0 = 8.903$ GHz; B_m (G) = 3230. Bottom: $\nu_0 = 8.702$ GHz, B_m (G) = 3170. The dashed lines in the bottom spectra are proton *s*-lines, simulated with the following parameters: $a_0 = 0$, $\mathbf{z}_h \equiv \{0.583, 0.694, 0.423\}$, $T = 8$ MHz. The lines observed in the low-frequency region (0−7 MHz) of all the spectra are believed to result from interaction of Mo^V with remote nitrogen(s) and are not discussed in this paper.

interaction must first be removed. Figure 3 gives an example of how this was achieved using a procedure similar to one utilized previously.[40,41] First, the original time-domain patterns of the *Pi* and *hpH* forms (Figure 3a, curves 1 and 2) were adjusted for relaxation decay and normalized to unity (see Figure 3b). Second, the ratio of the normalized time domains was obtained, as shown in Figure 3c. Finally, this resulting time domain was subjected to FT transformation (Figure 3d). The excellent effectiveness of this procedure is well demonstrated by the complete suppression of the lines from the remote matrix protons, present in equal amplitudes in both *Pi* and *hpH* forms (cf. Figure 2). Additional examples of FT spectra obtained at the various magnetic fields are included in the Supporting Information. As previously noted by Mims,[41] this procedure for extracting the desired deuterium modulation from the background does not strictly follow ESEEM theory. Equation 11 implies that modulation from numerous nuclei is the average product of the time domains and not a product of the averages. However, since the amplitudes of both the desired and background modulations are small, such a departure from strict theory leads only to an incorrect accounting of harmonics as a result of multiplying the corresponding cosines in eqs 9 and 11 and to a small additional error (∼2−3%) in the normalized ESE amplitude. Neither of these affects the present discussion. The opportunity to use this procedure for removing the background modulation was also one of the reasons for choosing a higher operational frequency.

The FT spectrum of Figure 3d consists of a set of rather broad merged *f*-lines, situated around ω_D, and a much narrower well-resolved *s*-line in the vicinity of $2\omega_D$. The ratio of the amplitudes for the *f*- and *s*-lines is not 4:1 but rather varies with field position from ∼1.5:1 to ∼0.6:1. This behavior is quite characteristic of strong anisotropic *hfi* and is therefore direct evidence of deuteron(s) near the Mo^V center. Splitting of the *f*-lines varies from ∼0 to ∼1.5 MHz (see Supporting Information) where the variation may be considered as the magnitude of the anisotropic *hfi*. Depending on field position, the amplitude of the *s*-line varies within the limits ∼6−8%, and this dependence is presented in Figure 4 along with the field-ESE spectrum.

On the basis of the absolute intensity of the *s*-line (see eqs 5 and 8), it is clear that there are between 1 and 4 (depending on their corresponding distances) D nuclei near the Mo^V. In addition, using the PDA we may immediately estimate the distance between Mo^V and D to be 2.1−2.5 Å, on the basis of the magnitude of the anisotropic interaction. A Mo−D separation of 2.1−2.5 Å would be expected in a Mo−O−D moiety; therefore, on a qualitative level, the simple 2-pulse ESEEM experiment sufficed to demonstrate conclusively that the *hpH* form of SO does have at least one nearby deuteron. To get more quantitative information it was necessary to analyze and fully simulate the intensity, shifts, and quadrupole splitting dependence of the *s*-line on magnetic field. The intensity of the ESEEM in the weak quadrupole interaction limit is determined only by the *hfi*; as we already mentioned, the *nqi* does not alter the ESEEM intensity explicitly. However, the *nqi* does change the line shape, which changes the apparent intensity. The anisotropic *hfi* can also affect the direction of quantization of the nuclear spin, which makes simulations of line shapes and absolute intensities a cumbersome iterative procedure.

As mentioned above, in principle the anisotropic part of the *hfi* may be found from the shifts of the *s*-line from the double Larmor deuteron frequency and the *nqi* parameters determined from the splitting of this line. In practice the *nqi*-induced broadening and lower spectral resolution for deuterons necessitated the use of a four-pulse experiment to obtain enough resolution for this purpose. Typical time-domain data collected in four-pulse experiments are shown in Figure 5. The maximum modulation amplitude was found around $\tau \approx 290-320$ ns, which is not too far from where optimal modulation conditions are found for matrix deuterons (e.g., $\tau \approx 340$ ns for the *Pi* sample). However, for the *hpH* form the modulation amplitude is about five times greater than for the *Pi* form (compare Figure 5, top, with Figure 1b), and admixture of modulation caused by matrix deuterons may be neglected. Representative FT spectra of the four-pulse time-domain data, collected at particular magnetic

(40) Lorigan, G.; Britt, R. D.; Kim, J. H. Hille, R. *Biochim. Biophys. Acta* **1994**, *1185*, 284−294.

(41) Mims, W. B.; Peisach, J. In *Advanced EPR Applications in Biology and Biochemistry*; Hoff, A. G., Ed.; Elsevier: 1989; pp. 1−55.

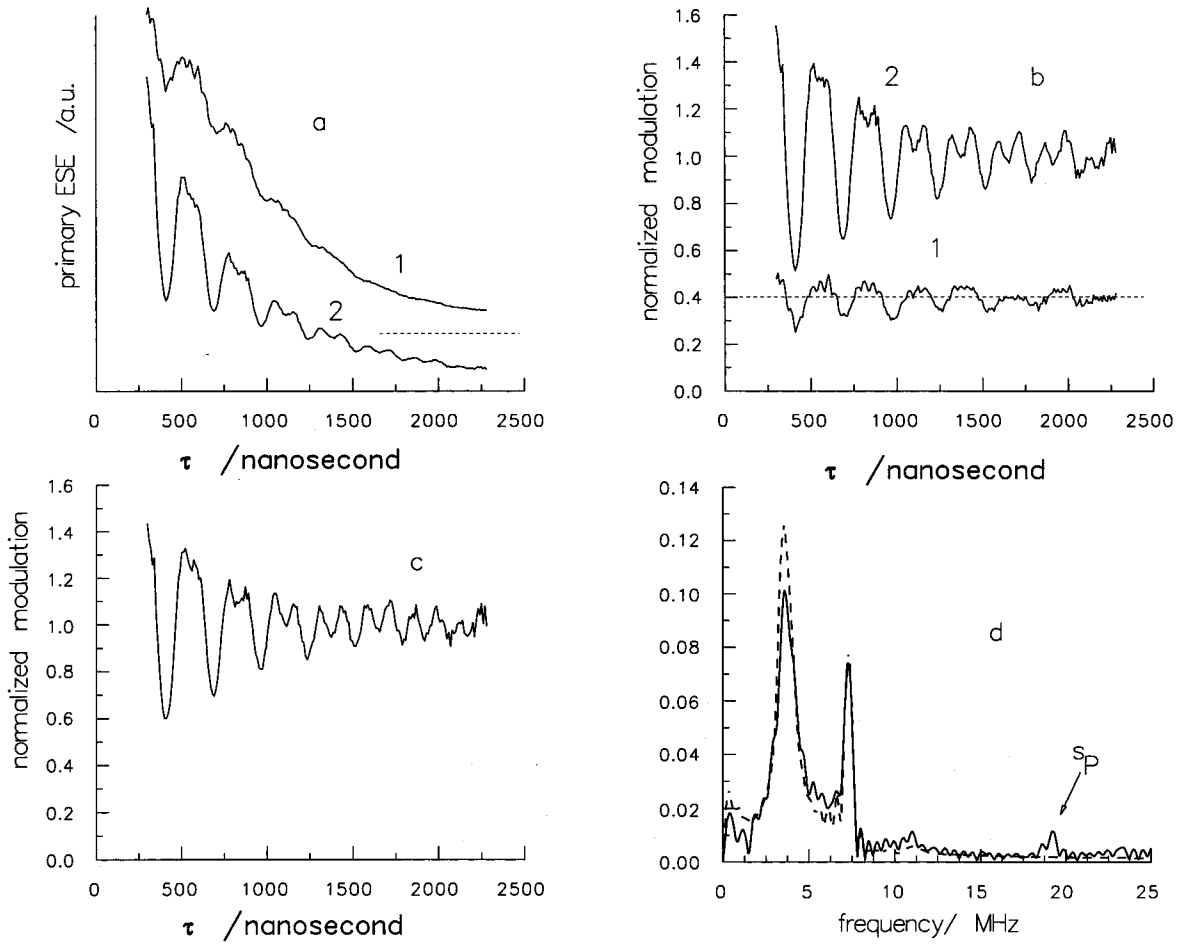

Figure 3. (a) Experimental time domains of the *Pi* (1) and *hpH* (2) forms of SO in D_2O. B_m = 5474 G, ν_0 =15.300, and 15.237 GHz for 1 and 2, respectively. Both curves are presented on the same scale; the dashed line is the zero for curve 1. (b) Time domains shown in a after adjusting for relaxation decay and normalization; curve 1 is shifted 0.6 units relative to curve 2. (c) Result of dividing curve 2 into curve 1 after the normalization. (d) FT spectrum of c (solid line) and its simulation (dashed line). Note that the spectrum shows a P-related peak, but no proton related peaks are present because their signal is canceled out by the division procedure. Parameters for simulation: a_0 = 0.3 MHz, T = 1.24 MHz, $\mathbf{z}_h$ = {0.583, 0.694, 0.423}, $\mathbf{z}_q$ = {0.91, 0.42, 0}, q_0 = 0.09 MHz, η' = 0.1. Additional FT spectra collected at other magnetic field strengths appear in the Supporting Information.

field positions, are shown in Figure 5, bottom. Similar spectra were obtained at 5−10 G intervals throughout the entire CW EPR line. The *s*-lines observed in these spectra were singlets between g_z and g_y, showing that the quadrupole splitting over this entire magnetic field interval is less than 0.14 MHz (the resolution dictated by the $t/2$ interval of 7 μs which was used in this experiment). Between g_y and g_x the *s*-line becomes a resolved doublet, with splitting which varies from 0.18 to 0.24 MHz, depending on the field. The behavior of the quadrupole splitting in the *hpH* form is thus quite different from that of the *Pi* form, which is independent of field. Moreover, the maximum value of the splitting in the *hpH* form (0.24 MHz) is significantly smaller than that of the *Pi* form (0.34 MHz). Finally, note that the center of the *s*-line of the *hpH* form is shifted from the double deuteron Larmor frequency by $\delta' \approx 0.18-0.24$ MHz, throughout the CW EPR spectrum. The magnitude of the shift allowed us to immediately evaluate a characteristic value for the anisotropic interaction (see eq 6) as $T \geq {}^4/_3\sqrt{\omega_D \cdot \delta'} \approx 1.15-1.3$ MHz. Comparing these data with splittings of the *f*-lines observed in the two-pulse spectra, we can conclude that the isotropic part of the *hfi* is likely also be within the range $|0-1.3|$ MHz.

It was previously shown that, for systems with an isotropic **g** tensor, the magnitude of the isotropic and anisotropic *hfi* can be obtained simultaneously by analyzing the contour plot from a HYSCORE experiment.[42] A HYSCORE experiment was carried out at one of the most nonselective orientations, near the g_y field position, but the contour plot was not informative, perhaps because even at this field position the ESEEM experiment still was orientationally selective. However, a projection of the HYSCORE spectrum on one of the frequency axes (Figure 6) reveals the clearly recognizable spectrum of a "dipolar powder pattern", from which the magnitude of the anisotropic interaction may be evaluated to be 1.2 MHz, in close agreement with the evaluations of the anisotropic *hfi* obtained from the 4-pulse experiments. According to eqs 5 and 8, a single deuteron with an anisotropic interaction of this magnitude can provide *s*-line intensities at a given operational frequency of as much as 20%; this value is 2.5× greater than the 8% maximum value observed experimentally. From this comparison, we hypothesize that the *hpH* form of SO possesses only a single deuteron within ∼3 Å of the Mo, most likely in the form of a Mo−OD moiety. To further probe this hypothesis, we have simulated the *s*-line intensity dependence on magnetic field, using an axial *hfi* tensor, a slightly nonaxial *NQCT*, and varying magnitudes of q_0, T, a_0, and the asymmetry parameter η',[33] as well as variable orientations of the *hfi* and NQC tensors in the *g* frame. Before discussing the results of these simulations, we

(42) Dikanov, S. A.; Bowman M. K. *J. Magn. Reson.* **1995**, *A116*, 125−128.

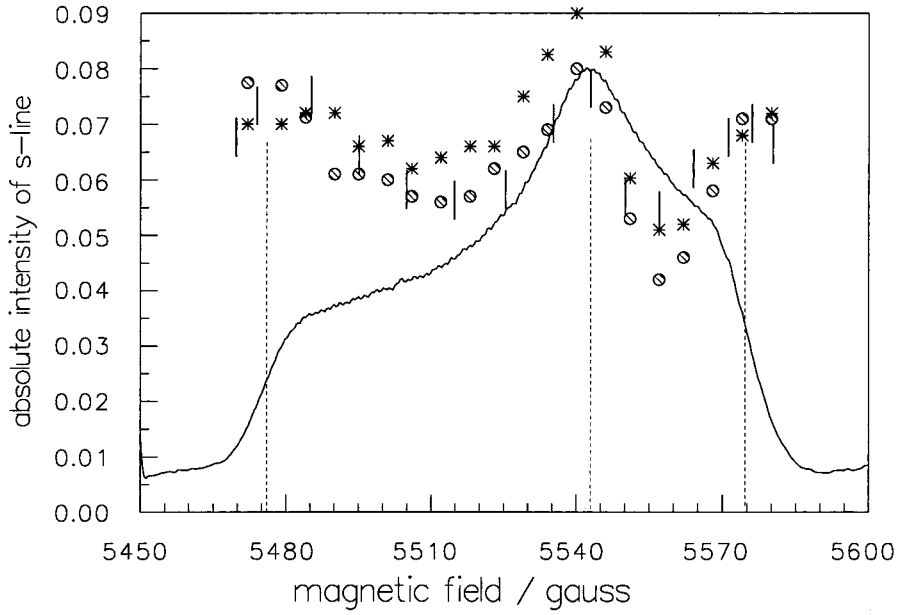

Figure 4. Dependence on applied magnetic field of the experimental (bars) and simulated (circles and asterisks) amplitudes of the *s*-line for a sample of the *hpH* form of SO in D_2O at $\nu_0 = 15.237$ GHz; the solid line is the corresponding field ESE spectrum. The principal *g* values evaluated from this spectrum are 1.988, 1.964,1.953 (compare with ref 12) and shown by dashed lines. Parameters used for the simulations: (circles) $\mathbf{z}_h \equiv \{0.583, 0.694, 0.423\}$, $T = 1.24$ MHz, $a_0 = 0$, $\mathbf{z}_q \equiv \{0.94, 0.34, 0\}$, $\eta' = 0.1$, and $NQCC = 0.09$ MHz; (asterisks) random distribution of T within the limits 1.15−1.3 MHz, with simultaneous random distribution of $\mathbf{z}_h$ in the *ZY* plane of the RCF, within the limits 59−77°, at a constant angle between $\mathbf{z}_h$ and *X*.

allow ourselves two comments. First, from the evaluated anisotropic interaction, one may easily estimate (using the PDA) the distance between Mo^V and the deuteron to be 2.2 Å, which is shorter than one would expect from simple geometrical evaluations[43] (Mo−O 2.2 Å, O−H 1 Å, angle Mo−O−H 109−116°, Mo−H distance 2.5−2.6 Å). Since Cramer et al. already reported a rather large spin-density on ^{17}O in the *hpH* form,[11] such a difference is expected when applying the simplest form of PDA and does not contradict the assumption that Mo^V coordinates an OH group. As for q_0, from the largest splitting of the *s*-line observed at g_x, assuming that $\mathbf{z}_q$ is close to the *x* axis of the RCF, and setting ψ in eq 10 to zero, one may evaluate it as 0.08−0.09 MHz. Such a small q_0 is quite unusual for water or an OD group coordinated to a metal ion;[30] indeed, the value of 0.18 MHz, found by Dikanov et al.[38] for a D-atom stabilized in glassy water/acid solution, was the smallest value for this parameter which had previously been found. Although worthy of future study, the problem of which type of charge distribution could give rise to such an unusually small *NQCT* parameter is far outside the scope of this paper. Henceforth, we will treat the *nqi* in a formal way without attempting to physically interpret the q_0 and *NQCT* orientations obtained from the simulations.

The small quadrupole splitting observed in this particular system has almost no effect upon the amplitudes of the *s*-lines in two-pulse experiments because the finite time interval results in a broadening of 0.5 MHz, which exceeds the quadrupole splitting. Therefore, as a first step in simulating the two-pulse data, only the *hfi* parameters were varied, and q_0 was set to zero. In this way, it was possible to simulate the field dependence of the *s*-line amplitude with just one iteration (see below). Subsequently, the observed field dependence of the quadrupole splitting could be simulated while maintaining the *hfi* parameters fixed at the values obtained in the two-pulse experiment. After q_0 had been refined, the *hfi* parameters were submitted to a slight final adjustment.

The preliminary evaluations of the range of T and a_0 also simplified the full simulation procedure. The value of a_0 is small, ($a_0/2 \ll \omega_D$), and it is well-known[26] that a small isotropic interaction does not significantly affect the amplitude of the *s*-line in simulations. Therefore, we mainly used an $a_0 = 0$. In addition, because the intensities of the *s*-line at the g_x, g_y, and g_z positions are comparable, the $\mathbf{z}_h$ vector should form approximately equal angles with the *x*, *y* and *z* axes of the RCF.

Using the above considerations as guidelines, repeated trial simulations eventually yielded a single set of parameters which reproduced both the experimental field dependence of the *s*-line intensity and its shifts from the double Larmor frequency, reasonably well. The final parameters were: $\mathbf{z}_h = \{0.583, 0.694, 0.423\}$; $T = 1.24$ MHz; $\mathbf{z}_q = \{0.94, 0.34, 0\}$, $\eta' = 0.1$ and $q_0 = 0.09$ MHz. A simulated intensity dependence of the primary echo *s*-line on field is shown in Figure 4 (circles), and Figure 5 gives an example of simulated four-pulse line-shapes. The simulation of the primary echo dependence was quite sensitive to $\mathbf{z}_h$ orientation, i.e., a change as small as ±5° in the $\mathbf{z}_h$ projection on the RCF *z* axis from the nominal value results in a noticeably poorer match to the experimental data. Variation of the magnitude of the anisotropic part of *hfi* with other parameters fixed resulted in T^2 dependence of amplitudes and shifts (see eqs 3 and 5). On the other hand, the simulations were not sensitive to variation of a_0 within the limits 0−0.4 MHz, and because the absolute magnitude of the *nqi* was small, they were not very sensitive to variation of the *nqi* parameters; e.g., one may vary η' within the limits 0−0.1, q_0 within the limits 0.08−0.1 MHz, and $\mathbf{z}_q = \{0.94-0.87, 0.34-0.5, 0-0.2\}$ (keeping of course $|\mathbf{z}_q| = 1$) without significantly affecting the fits. With this set of anisotropic *hfi* and *nqi* parameters, we were also able to reproduce with reasonable accuracy the shapes and absolute intensities of the *f*-lines in the two-pulse spectra, as shown in Figure 3d and Supporting Information. However,

(43) Bohmer, J.; Haselhorst, G.; Wieghardt, C.; Nuber, B. *Angew. Chem., Int. Ed. Engl.* **1994**, *33*, 1473−1476.

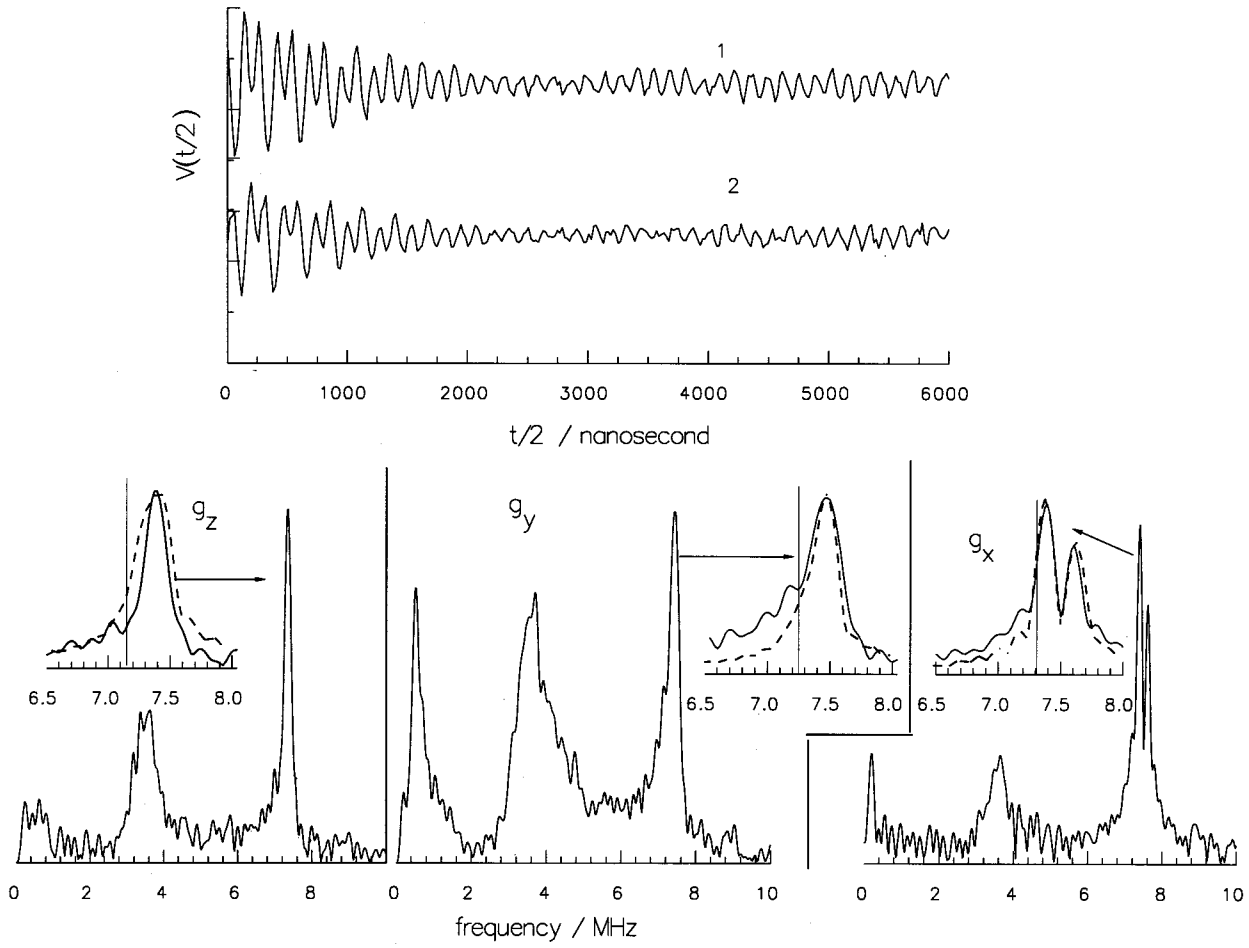

Figure 5. (Top) Time-domain four-pulse ESEEM of the *hpH* form of SO in D_2O, collected near the g_x position. For curves 1 and 2 τ is 310 and 290 ns, respectively. Experimental conditions: $B_m = 5571$ G, $\nu_0 = 15.237$ GHz. Note that the scale in this figure is the same as that in Figure 1b. (Bottom). Four-pulse FT spectra of the *hpH* form at various magnetic fields, corresponding to the g_z, g_y, and g_x positions. From left to right B_m (G) = 5474, 5543, 5576, respectively. The time domains for these spectra were collected using a total of 300 steps with $t/2$ of 23 ns. The inserts are enlargements of the *s*-lines in the corresponding spectra (solid lines) and their simulations (dashed lines); the simulation parameters are the same as those used in Figure 4, circles. The vertical lines in the inserts mark the position of the double Larmor deuteron frequency at each of the given fields.

to get a good match in these simulations, we had to use different values of a_0 (but still within the limits 0−0.4 MHz), depending on field position. Such adjustments of a_0 might seem somewhat arbitrary; however, there is a probable explanation for why a_0 should be field-orientationally dependent, to which we return below in our analysis of data obtained for the *hpH* form of SO in H_2O.

The analysis thus far succeeds in fitting all of the ESEEM data for the *hpH* form of SO in D_2O to a model of one nearby deuteron with a definite set of magnetic resonance parameters. Unfortunately, such a model does not work when applied to the *hpH* form of SO in H_2O. The dashed line shown in Figure 2 (bottom) represents the proton *s*-line simulated with the same *hfi* parameters that were used in the above simulations but recalibrated for a proton instead of a deuteron. This line is well separated from the *s*-line related to matrix protons, and for some field positions its amplitude exceeds that of the matrix proton line and should be easily observed experimentally, if present (see Supporting Information). The fact that no lines are observed experimentally indicates that the coordinated group must have a distribution of *hfi* parameters, which would cause a loss of amplitude. The concept of a *hfi*-parameter distribution has already been utilized elsewhere to explain ESEEM spectra of organic radicals and metalloenzymes.[15,38,39] Experimentally, it is taken to indicate that the coordinated group in question does not have a unique orientation in the molecular frame; this could well result in a distribution of directions for the principal axis of the *hfi* tensor and also in variable magnitudes for the isotropic and anisotropic parts of the *hfi*. Generally, taking into account the usual ESE problem with complete excitation of proton *hfi* transitions, a proton *s*-line amplitude should be suppressed by a factor of 5−6 to be comparable with the noise level. We tried to find some distributions that would cause such an amplitude loss yet still describe the dependencies obtained for deuterated samples, and we have partially succeeded in solving this problem. For instance, a two-dimensional uniform distribution centered at the previously used unique orientation (variation of $\mathbf{z}_h$ relative to the *z* axis of the RCF within the limits 59−76°, at a constant angle between $\mathbf{z}_h$ and *X*, and *T* variation within the limits 1.15−1.3 MHz) reproduces the field dependence of the *s*-line amplitude for deuterated samples reasonably well (see Figure 4, stars), and results in the desired 5-fold decrease of the proton *s*-line. This distribution does not, however, reproduce the amplitudes and shapes of the *f*-lines (for the deuterated samples). Additional evaluations showed that matching the *f* -lines would require an associated variation of the isotropic/anisotropic interaction, a cumbersome problem involving the determination a large parametric distribution with associated parameters. This is a whole project in its own right and beyond of scope of this paper; nevertheless, our numerous

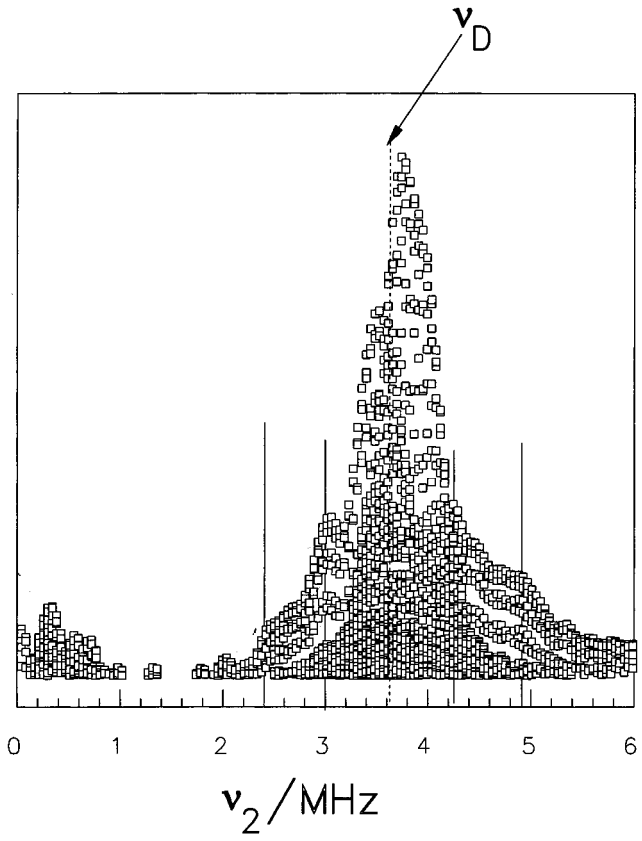

Figure 6. Projection of the HYSCORE spectrum of the *hpH* form on one of the frequency axes. The dashed line marks the deuteron Larmor frequency at the given field. The solid lines mark peaks and shoulders of the assumed dipolar pattern. Note that the distance between shoulders is twice as large as between peaks and that they are symmetrical relative to ν_D. Experimental conditions: $\nu_0 = 15.249$ GHz, $B_m = 5550$ G ($g = 1.963$), $\tau = 320$ ns.

simulations did make it clear that we are quite restricted in how we may vary the parameters. In effect, the coordinated group is still essentially oriented relative to the Mo^V center. Therefore, the necessity of varying a_0 (at constant magnitude of anisotropic *hfi*) when simulating the deuterium *f*-lines to match experiment might be simply an additional indirect clue of the existence of such an associated distribution. Also, it may be worth noting that the angle between $\mathbf{z}_h$ and $\mathbf{z}_q$ (40−45°) is within the limits expected from the known geometry of Mo−O−H bonds. Yet as we mentioned above, that correspondence may be just accidental, since $\mathbf{z}_h$ could deviate from the direction of the Mo−H vector; the unusually small magnitude of q_0 keeps us from the temptation of considering the $\mathbf{z}_q$ direction as the direction of the OH bond, as previously reported.[30] Finally, we should also stress that the introduced distribution is not a unique solution of the problem, and the parameters that we derived show only the range of allowed parameter variation. The important point is that, as one can see, the range of these variations is not large.

Therefore, concluding this section, we can state that Mo^V in the *hpH* form of SO definitely coordinates a group that includes one D(H), probably in the form of a Mo−OH(D) moiety. The orientation of this group is not fixed (although it is substantially restricted) and thus gives rise to a distribution of *hfi* parameters. The resulting loss of amplitude makes impossible the direct observation of a ^{1}H line using ESEEM; however, such a line is observable in ESEEM spectra of the comparable deuterated enzyme because the smaller gyromagnetic ratio of deuterium leads to a smaller *hfi* distribution. Note that the observed distribution of *hfi* parameters should also make impossible the direct observation of a ^{1}H line using the CW EPR technique previously reported by George,[17] which suggests that the signals he observed were due not to a coordinated Mo−OH but to more distant exchangeable protons which in our case merged with the matrix line.

Low-pH Form. The *X*-band CW EPR spectra obtained for the *lpH* form of SO (in H_2O or D_2O) had the expected appearance, based on the previous literature; the sample in H_2O showed proton splitting, and the principal *g* values, $g_z = 2.004$, $g_y = 1.972$ and $g_x = 1.966$ were close to the published values.[12]

Two-pulse ESEEM spectra of a SO sample in H_2O exhibit a deep low-frequency modulation as expected for interaction of Mo^V with a SC proton under conditions of partial excitation of the *hf* transitions.[44] For the sake of comparison, a representative example of the *lpH* ESEEM pattern is shown in Figure 7a, along with that of the *Pi* form, in which such low-frequency modulation is absent. Note that, except in this respect, the proton-related modulation is quite similar in magnitude in the two forms. The FT spectra, presented in Figure 7 b−d consist of *f*- and *s*-lines, situated at the proton and double proton Larmor frequencies; the absolute intensities of these lines do not depend on magnetic field. Therefore, as we mentioned in the Introduction, any additional proton interaction other than that already known from CW EPR was not observed. However, we already demonstrated in our discussion of the *hpH* form that even a slight disorder in Mo−H orientation can give rise to a distribution of *hfi* parameters sufficiently broad that the resulting proton modulation is no longer visible. To investigate the possibility of a second nearby proton in the *lpH* form, we performed a detailed investigation of deuterated samples, analogous to our *hpH* investigation.

For *lpH* SO in D_2O, the *hfi* with the SC deuteron is reduced, and complete excitation of *hfi* transitions can be achieved. However, this creates difficulties for the present study because the spectrum originating from Mo interaction with the SC deuteron will certainly overlap with the spectrum from a putative second deuteron. Fortunately, the parameters of the *hfi* tensor for the SC deuteron are already known with EPR accuracy, and these can be used as a starting point for evaluations and simulations. Therefore, all of the experiments and simulations described below were aimed at understanding whether we could describe the observed ESEEM spectra with the assumption of just one SC proton or whether coordination of a second proton needed to be invoked.

We start with the two-pulse ESEEM data. Background modulation was removed by the same procedure that was applied to the *hpH* form; the resulting normalized time domains for two different field positions together with their FT spectra are shown in Figure 8. As one can see, the FT spectra consist of two *f*-lines and an *s*-line. A striking feature of the spectra, observed at all field positions, is a "window", centered at about ω_D, where no signals are detected. This window is a result of selecting the optimum operational frequency (15.3 GHz) for this experiment. At typical *X*-band frequencies only a single broad feature is observed because of cancellation and the lower Larmor frequency of D. The variation of the *s* -line amplitude was thoroughly investigated across the CW EPR spectra, and the results are shown in Figure 9 along with the associated field ESE spectra. As one can see from Figure 9, the amplitude depends strongly on magnetic field; it is minimal at g_z (<1%), reaches a maximum value of 5% between g_z and

(44) Evelo, R. G.; Dikanov, S. A.; Hoff A. J. *Chem. Phys. Lett.* **1989**, *157*, 25−30.

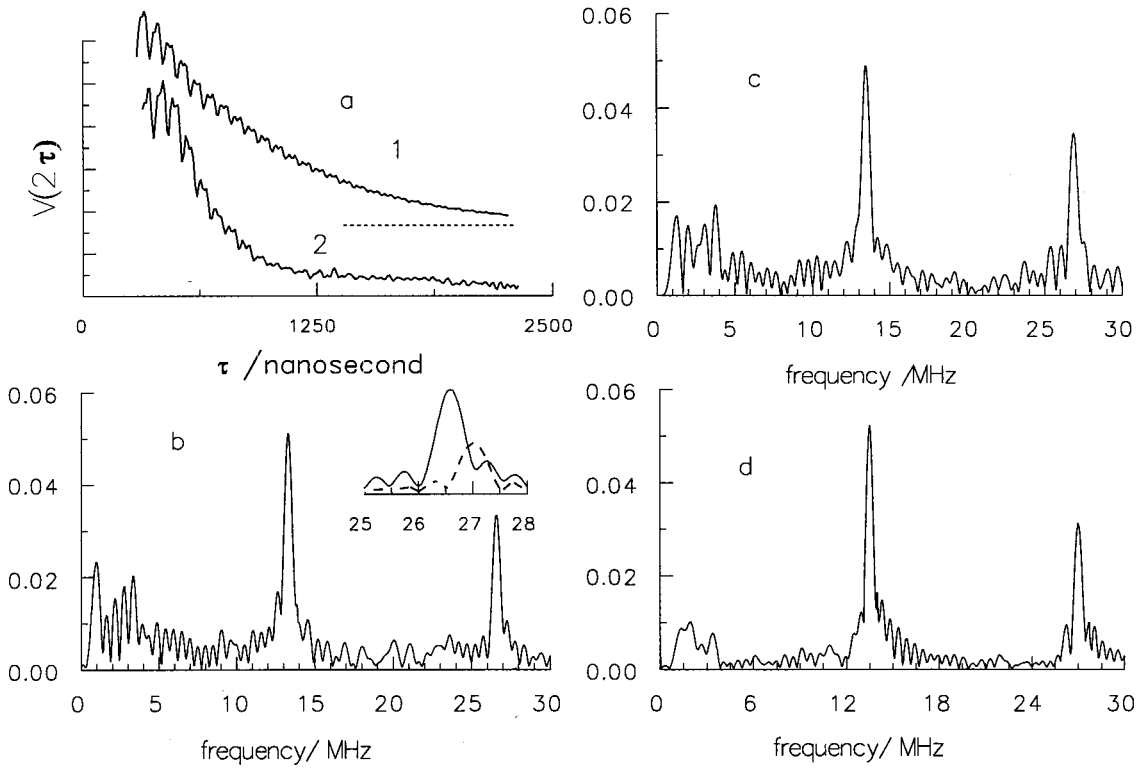

Figure 7. (a) Two-pulse time domain ESEEM of the *Pi* (1) and *lpH* (2) forms of SO in H_2O. Experimental conditions: $B_m = 3220$ and 3120 G, $\nu_0 = 8.9$ and 8.7 GHz, for 1 and 2, respectively. (b)−(d) Normalized FT spectra of the *lpH* SO form in H_2O at various field positions; B_m(G): (b) 3120, (c) 3150, (d) 3165. Low-frequency modulation in all the spectra was removed during the course of normalization. Inset: (dashed) *s*-line expected for a second proton and simulated with $r = 3$ Å and $\mathbf{z}_h = \{0.57, 0.82, 0\}$ and $a_0 = 7.8$ MHz; (solid) enlarged experimental *s*-line, presented on the same scale as the simulated line.

g_y, and decreases to 2.5−3% at g_x. In accord with eq 5 and the known *hfi* tensor, an upper limit of 5.5−11% can be placed on the theoretical *s*-line intensity resulting from interaction of Mo^V with a SC deuteron, depending on the impact of quadrupole splitting on line shape. The maximum observed experimental value of 4.7 ± 0.3% is below the low limit of this evaluation, supporting the hypothesis of one nearby deuteron. Since more accurate evaluations have to include the quadrupole interaction, we utilized the four-pulse technique to investigate the quadrupole splitting of the *s*-line over the entire EPR spectrum.

Figure 10 presents four-pulse time-domain data collected near the g_y position, with $\tau = 240$ and 340 ns. In contrast with data obtained for the *Pi* form (Figure 1), in which modulation is hardly detectable at $\tau = 240$ ns, the data for *lpH* SO show very noticeable modulation (indeed, maximum modulation occurs at this particular τ). This experiment allowed us to conclude that the observed modulation pattern at $\tau = 240$ ns originates solely from interaction of Mo^V with nearby nuclei, without interference from background modulation. What is more, at the given τ, only one nucleon is responsible for the modulation. Indeed, in a HYSCORE experiment, in which the *f*-line amplitudes have the same τ-dependencies as the *s*-line amplitudes in the four-pulse experiment, only two correlated hyperfine frequencies, split by *nqi*, are observed at $\tau = 240$ ns (Figure 11). As one can see from Figure 11, the fundamental frequencies found from the contour plot are $\omega_\alpha \approx 5.6$ and $\omega_\beta \approx 1.9$ MHz. EPR lines at this field position should be split by $\omega_\alpha - \omega_\beta \approx 3.7$ MHz (24 MHz or 8.7 G for a proton), which is in a good agreement with published data ($A_y = 8$ G).[12] Therefore, the four-pulse time domains are considered to be modulations from one nucleon. As one can see from Figure 10, the *s*-line is a doublet. The splitting ranges from 0.34 to 0.36 MHz at the g_z and g_y field positions, to 0.64−0.66 MHz at the g_x position. More complicated line shapes were observed at intermediate magnetic fields (see Supporting Information). The field dependence of the quadrupole splittings over the entire CW EPR spectrum is shown in Figure 12. From the four-pulse experiment, we also extracted the shift of the center of the *s*-line from the double Larmor deuteron frequency. The maximum magnitude of this shift was 0.15−0.17 MHz. Note that unlike what was observed for the *hpH* form, the *s*-line quadrupole splitting magnitudes in this case are quite close to those observed in similar compounds.[18] From the above information, we may immediately evaluate the directions of the *NQCT* axes of the SC deuteron and q_o, using the splittings at just the three canonical orientations. The splittings vary by approximately a factor of 2 when the external magnetic field varies from one canonical orientation, g_z, to another, g_x. As follows from eq 10, one may expect such a variation if $\mathbf{z}_q$ is close to the *x* axis of the RCF; indeed, at $\eta' = 0$ a 2× increase in splitting accompanies a shift of ψ from 90° (the g_z position, $B_m \| Z$) to 0° (the g_x position, $B_m \perp Z$ and $\| X$). As we already discussed above, a q_o which is consistent with all three splittings is 0.2−0.24 MHz, which is a typical value reported for coordinated D_2O or OD.[30] We will now use these estimates as a starting point in full simulations.

As already mentioned, a quantitative data interpretation involves the simultaneous simulation of the *s*-line intensity dependence, found in the two-pulse experiments, and the dependence of the quadrupole splittings and line shapes on field, found in the four-pulse experiments. To proceed with the simulation, we have to know not only the principal values of the SC deuteron's *hfi* tensor but also its orientation in the RCF. This orientation was not specified in the paper of Lamy et al.,[12] but on the basis of their published data, one would initially assume that $\mathbf{z}_h$ is parallel to the *x* axis of the RCF. However, such an orientation of the *hfi* tensor immediately gives a zero

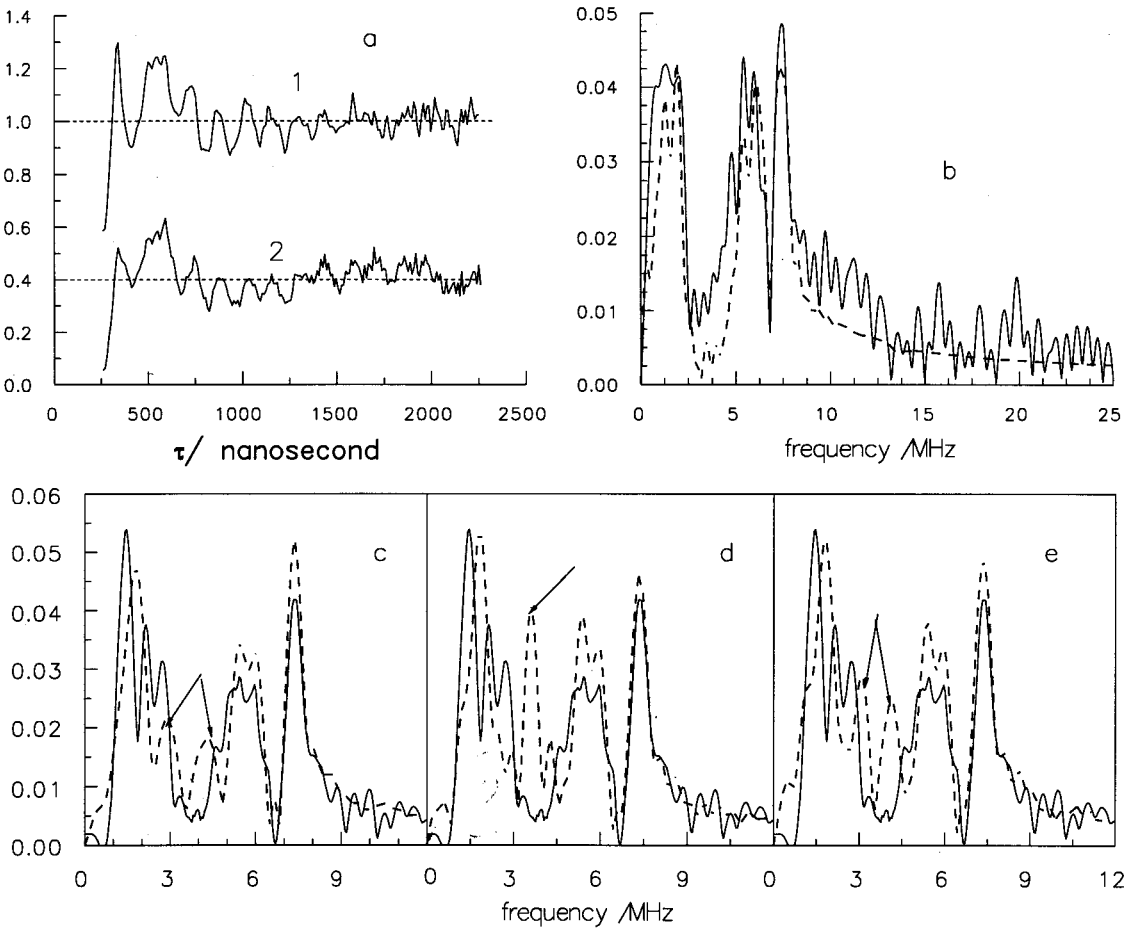

Figure 8. (a) Two-pulse normalized time domains (with matrix modulation removed) of the *lpH* form of SO in D_2O at B_m = 5548 and 5506 (curves 1 and 2, respectively). (b) FT of curve 1 (solid line) and its simulation (dashed line). (c)−(e) FT of curve 2 (solid lines) and their simulations (dashed lines). Simulation parameters: (b) a_0 = 4 MHz, axial anisotropic *hfi* $|T|$ = 0.79 MHz, $\mathbf{z}_h$ = {0.98, 0.14, 0.14}, $\mathbf{z}_q$ = {0.903, −0.42, −0.087}, *NQCC* = 0.225 MHz. Simulations in (c)−(e), also incorporate a second deuteron with parameters: r = 3 Å, $\mathbf{z}_h$ = {0.57,0.82, 0}, $\mathbf{z}_q$ = {0.105, 0.995, 0}, *NQCC* = 0.225 MHz, a_0 (MHz): (c) 1.2, (d) 0, (e) −1.2. Arrows in (c)−(e) show additional lines expected from a putative second deuteron. Time domains were collected at ν_0 = 15.300 GHz, using steps of τ = 10 ns, over a time interval 260−2260 ns.

intensity of modulation at the g_x and g_z positions. Experimentally (see Figure 9) the intensity of the *s*-line at the g_x position is indeed close to zero, but at g_z the intensity is still quite substantial. Such disagreement could be caused by the presence of a second deuteron, but it could also be caused by a slight misalignment between the RCF and the principal axis of the *hfi* tensor, which CW EPR simulations failed to recognize. Therefore, in simulations we allowed a slight departure of the *hfi* tensor axis from the RCF to satisfy the observed intensity dependence and a slight departure from the reported principal values to satisfy the observed shifts of the *s*-line from the double deuteron Larmor frequency. None of these minor variations of the *hfi* tensor exceed the limits of experimental CW EPR accuracy. As a result of numerous simulations, we ended up with an axial hyperfine tensor with the parameters (for a proton): a_0 = 26 MHz, $|T|$ = 5.12 MHz and $\mathbf{z}_h$ = {0.98, 0.14, 0.14}. In selective g_x and g_z orientations, such *hfi* splits the EPR line by 35.5 MHz (12.9 G) and 21.3 MHz (7.6 G) respectively, in good agreement with the experimentally observed splittings, as well as with published data.[12] Actually, mutual constraints imposed by CW EPR and spin−echo measurements in combination do not leave much room for variation of these parameters nor is there much freedom for varying the *nqi* parameters when fitting the field dependencies of the quadrupole splittings and line shapes, observed in the two- and four-pulse measurements. Namely, q_0 may be varied within the limits 0.22−0.23 MHz, η' within the limits 0.06−0.12, and $\mathbf{z}_q$ within the limits {0.91−0.87,(−0.42)−(0.5),(−0.1)−0.0} ($|\mathbf{z}_q|$ = 1). The calculated dependencies of *s*-line intensity (two-pulse experiment), quadrupole splitting (four-pulse experiment), and line shapes (both, two- and four-pulse experiments) for selected sets of parameters are shown in Figures 8, 9, 10, and 12. As one can see from Figure 8, which presents two-pulse spectra for two particular field positions, the simulations reproduce the spectra in their entirety, including both the *f*- and *s*-lines, within the limits of experimental accuracy. The simulation for two sets of parameter dependencies of *s*-line on field, shown in Figure 9, also fit experiment. Four-pulse line shapes were reproduced at practically all field positions; the only exception was found in intermediate g_y−g_x field positions where *nqi* results in a rather complicated line shape (see Supporting Information). In this particular case, experiment shows a less resolved triplet than the simulation; decreasing the asymmetry parameter gives a better fit, but exact matching could not be achieved. The reasons for this observed difference are not exactly clear; probably the theory that was applied in the simulations is still too approximate to reproduce the fine details of line structure observed at that particular field. Finally, Figure 12 shows that the experimental dependence of the *s*-line quadrupole splittings on field is also well simulated. Therefore, we may conclude that, neglecting minor deviations, all sets of

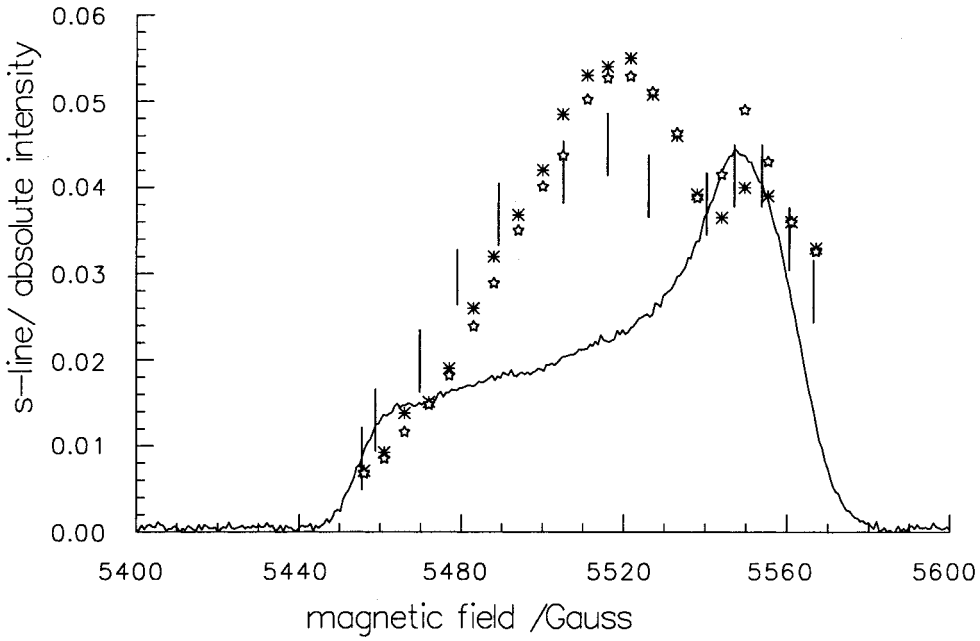

Figure 9. Field ESE spectrum (solid line) of the *lpH* form of SO and absolute intensity of the *s*-line: experimental (bars) and simulations (stars and asterisks). In the simulations: $a_0 = 4$ MHz; anisotropic *hfi* tensor is axial, with $|T| = 0.79$ MHz, $\mathbf{z}_h = \{0.98, 0.14, 0.14\}$, $NQCC = 0.225$ MHz, $\eta' = 0.12$, $\mathbf{z}_q = \{0.903, -0.42, -0.087\}$ (stars), and $\{0.906, -0.423, 0\}$ (asterisks).

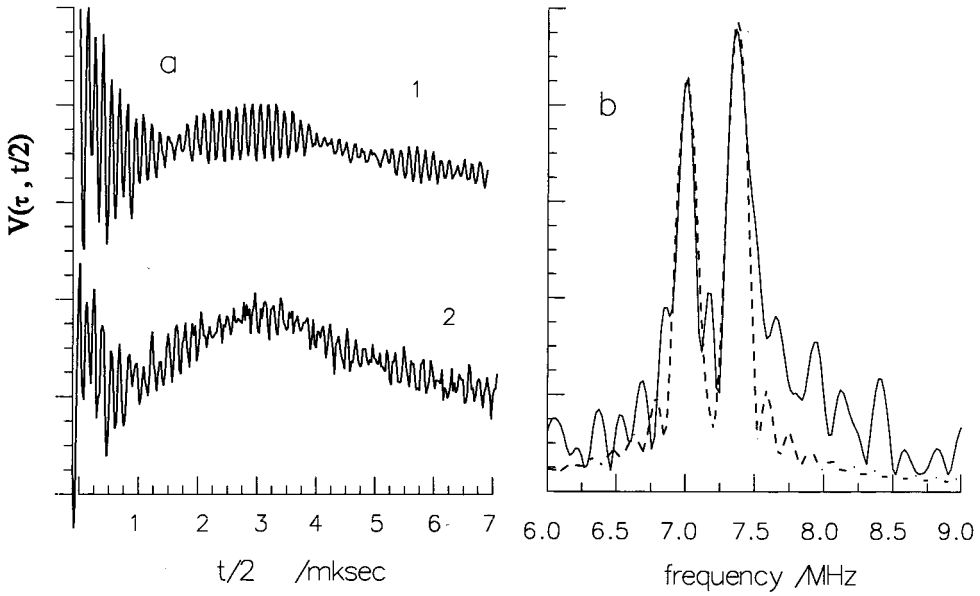

Figure 10. (a) Four-pulse time-domain of *lpH* SO in D_2O, collected at the g_y position; for curves 1 and 2, τ is 240 and 340 ns, respectively. Experimental conditions: $B_m = 5548$ G, $\nu_0 = 15.300$ GHz. (b) Experimental (solid line) and simulated (dashed line) four-pulse *s*-line shapes of *lpH* SO in D_2O at B_m (G) = 5455. Parameters of simulation as in Figure 9 (stars). Additional examples in Supporting Information.

experimental data are well-simulated using a model of one nearby proton (deuteron) with a unique set of parameters. We next used these parameters to evaluate an orientation for the SC deuteron in the RCF.

First of all, using the PDA, one finds that the distance between Mo^V and the SC deuteron, as calculated from the anisotropic part of the *hfi*, is ~2.5 Å, which is in rather good agreement with the distance of 2.5−2.6 Å known for Mo−O−D systems.[43] Also in the PDA, the direction of Mo−H coincides with the direction of $\mathbf{z}_h$ and $\mathbf{z}_q$, as we already mentioned, and is close to the direction of OD. The angle calculated between these two vectors is 33−35°, which is close to the 40−45° estimated from the known geometry of Mo−O−H bonds. It is surprising that the PDA works so well in a system with such a large isotropic constant as that found for the SC deuteron; nevertheless, the results allowed us the opportunity to evaluate the orientation of a possible second deuteron, assuming that both of them belong to the same water molecule. Having solved a simple geometrical problem based on the known geometry of water, we found that the distance from a putative second deuteron to Mo^V would be 2.7−3 Å and that the Mo-D vector would make an angle of ~60° with the *x* axis of the RCF and lie close to *XY* plane. These data immediately allow us to obtain the anisotropic part of the *hfi* for the putative second deuteron. The O−D bond direction for this deuteron was found practically parallel to the *y* axis and close to *XY* plane. The last parameter required for simulations is the isotropic constant. Indeed, since in the EPR spectrum splitting is observed only from one proton, the *hfi* of a second one would have to be less than the line width. The reported $^1/_2$ line width is ~8 MHz,[12] and therefore the

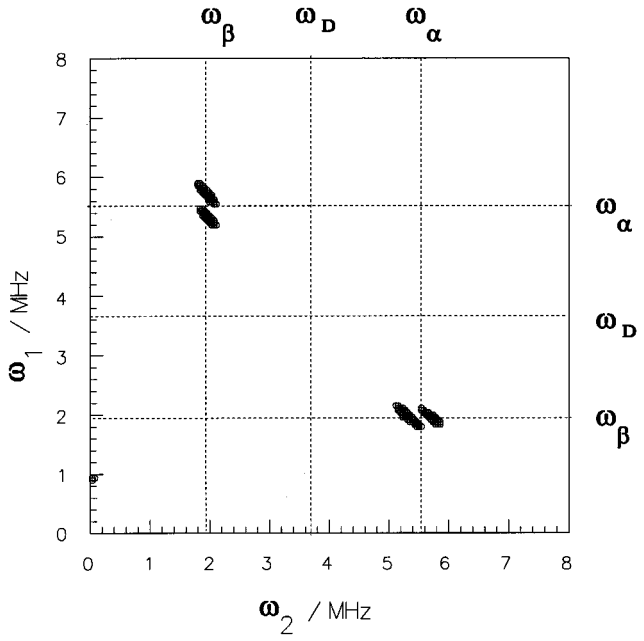

Figure 11. Projection of the experimental HYSCORE spectrum of *lpH* SO (in D_2O) on the $\omega_1-\omega_2$ plane. The marked contour delimits 90% of the maximal amplitude in the ++ quadrant. $B_m = 5552$ G, $\nu_0 = 15.300$ GHz. For all other parameters, see text. The frequencies of the *f*-lines and the D Larmor frequency are marked by dashed lines.

characteristic isotropic *hfi* of the second proton could not exceed this value, which corresponds to ~1.2 MHz for a deuteron. With these parameters, we performed a series of simulations of the two-pulse spectra which included both the SC deuteron and a second deuteron with the allowable characteristics just described. The magnitudes of the *s*- and *f*-lines belonging to a second proton would strongly depend on distance (as r^{-6}). Uncertainty in $\mathbf{z}_q$ and $\mathbf{z}_h$ orientation should not affect the maximum amplitude of these lines but rather result only in a variation in the field position where this maximum amplitude is found. Finally, the shape of the *f*-lines should strongly depend on variations of the isotropic constant within the allowed limits. Some results of the simulations are presented in Figure 8, which illustrate worst-case scenarios, a deuteron at the largest possible distance of 3 Å, with one of three isotropic constants, ±1.2 or 0 MHz. As one can see from Figure 8, even such a distant nucleon, if it had a zero isotropic constant, would be expected to give fairly prominent *f*-lines. In the simulations, they merge into one line with a peak intensity of 4% and are clearly seen in "the window" centered around the D Larmor frequency present in all of the spectra of the SC deuteron. The increase of the *s*-line intensities is not remarkable and is within the range of experimental accuracy. Although decreased in amplitude, the *f*-lines continue to be clearly visible when the isotropic constant does not exceed ±0.5 MHz. With further increases in the isotropic constant, the *f*-lines start to be obscured by those of the SC deuteron, and at the maximal allowable isotropic constant of 1.2 MHz, they would not be recognizable in the spectrum. Note, however, that they might still be detectable at $a_0 = -1.2$ MHz. We thus conclude that the possible presence of a second nearby deuteron cannot be completely ruled out on the basis of the available spectroscopic evidence; however, the possible parameter set for such a deuteron is severely restricted.

Utilizing the orientation for a putative second nucleon (vide supra), we simulated a spectrum expected for a sample of *lpH* SO in H_2O instead of D_2O. Since proton related *f*-lines are substantially broadened and therefore of much smaller amplitude than the *s*-line, only the latter will be discussed. As can be seen from Figure 7b (insert), the *s*-line from this proton should have an intensity of 1.7−1.8% and be shifted from the double proton Larmor frequency (and from the more intense *s*-line arising from remote protons) by ~0.5 MHz. Such intensity is within our limits of detectability, as we previously demonstrated in our investigation of P-related modulation in the *Pi*-form.[15] However, since experimentally observed proton-related modulations are typically 1.2−1.4× smaller than predicted by calculation (the reasons can be found elsewhere[45]), such a line could still be essentially obscured by the nearby *s*-line of matrix protons, whose amplitude is ~3%. In such cases, the resolution may be increased while at the same time suppressing the amplitude of the matrix *s*-line by utilizing the four-pulse technique with the appropriate τ-adjustment.[46,47] Moreover, the bigger the isotropic constant, the better the achieved improvement in resolution. We performed a four-pulse experiment on this sample and observed no additional *s*- line besides that assignable to matrix protons. Still, one experimental opportunity remains to check for the presence of a second nearby proton. This is to perform an experiment at the operational frequency of 3−4 GHz, which would increase the shift of the *s*-line (if present) from 0.5 to 1−1.5 MHz, and boost its intensity by 4−9 times. The desired operational frequency is out of the range of our present instrumentation; however, a planned instrument upgrade will allow us to perform this experiment in the very near future. For the moment, all of our experimental data supports the hypothesis of OH rather than H_2O coordination in the *lpH* form of SO. Moreover, the "worst-case scenario" geometry considered in our simulations assumes an O−H(D) bond length for the second nucleon which is unusually long for even a coordinated $H(D)_2O$. In addition, this geometry suggests that the Mo−OD_2 moiety is trigonal planar about the O, which is unlikely. If only more realistic geometries are considered, the possibility that a second nucleon is present but undetectable becomes even more remote.

Possible Geometrical Significance of the *hpH/lpH* Parameter Differences. The directions of $\mathbf{z}_q$ and $\mathbf{z}_h$ found for *lpH* and *hpH* SO cannot be directly compared because they were obtained in different RCFs, and neither the relation between these RCFs nor between the RCFs and the molecular frames is known. However, some general conclusions can be drawn about the relative Mo−H(D) interactions in each case. As mentioned earlier, the crystal structure of SO[7] and recent resonance Raman and ^{18}O-labeling experiments[21] suggest that of the two oxygen atoms coordinated to the Mo center (Structure **2**), it is the equatorial oxygen atom which is protonated in the Mo^V form of the enzyme. The rather large isotropic constant found for the *lpH* form and the rather large anisotropic constant found for *hpH* form also suggest that the proton in both forms is most likely coordinated to an equatorial oxygen.[48] A thorough single-crystal ENDOR investigation of a similar d^1 system, involving a vanadyl group with a coordinated water, previously showed that a small deviation of the metal-(equatorial proton) vector from the node of a singly occupied ground-state orbital results in a rather large variation of the isotropic constant, which can even change sign (−0.39 to +7.73 MHz).[48] Thus the large difference in a_0 (26 vs ~0 MHz) between the *lpH* and *hpH* forms of SO could be due simply to a relatively small displacement of the OH group (relative to the molecular frame),

(45) Astashkin, A. V.; Dikanov, S. A.; Kurshev, V. V.; Tsvetkov, Yu, D. *Chem. Phys. Lett.* **1987**, *136*, 335−340.
(46) Lee, H.; McCracken, J. *J. Phys. Chem.* **1994**, *98*, 12861−12870.
(47) Dikanov, S. A.; Spoyalov, A. P.; Hüttermann, J. *J. Chem. Phys.* **1994**, *100*, 7973−7983.
(48) Atherton, N. M.; Shackleton, A. J. *Mol. Phys.* **1980**, *39*, 1471−1485.

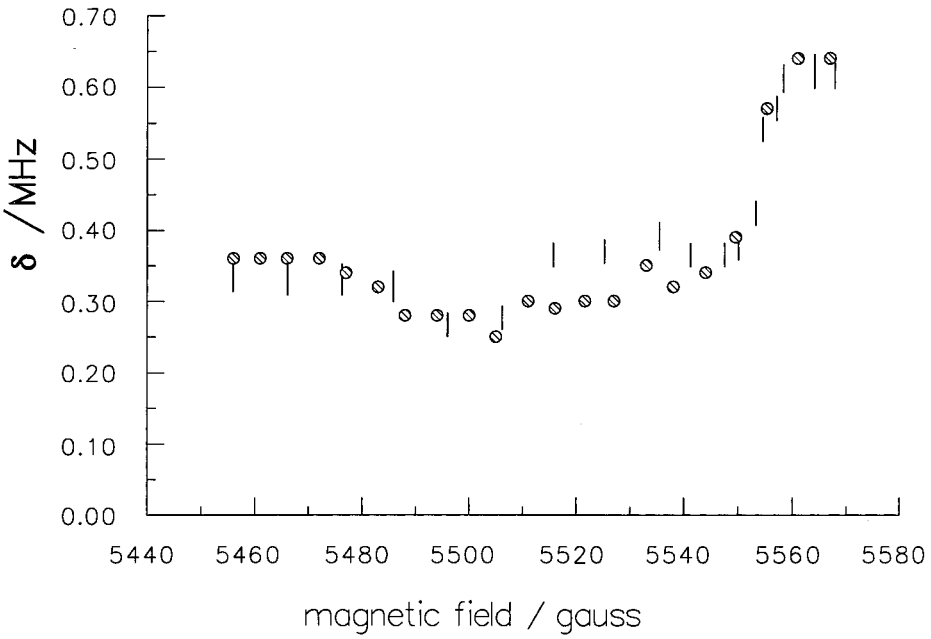

Figure 12. Experimental dependence of the quadrupole splitting of the *s*-line of *lpH* SO (in D_2O) on magnetic field (bars) and the corresponding simulation (circles). The parameters used for simulation were as for stars in Figure 9.

which moves the proton (deuteron) in and out of a node of the singly occupied d orbital. Very recent kinetic investigations in our laboratories suggest a mechanistic explanation for the *lpH*/*hpH* isomerization, consistent with such a displacement of the OH group.[10]

The geometries of the Mo^V-OH center proposed here for the *hpH* and *lpH* forms of SO are consistent with the crystal structure of chicken liver SO which shows a 5-coordinate approximately square pyramidal Mo center with a unique oxygen atom in the equatorial plane that is exposed to solvent and anions (**2**).[7,10] The remainder of the Mo site is buried within the protein, precluding coordination by a sixth ligand without major structural rearrangement at the Mo center. Previous EXAFS spectroscopy on the Mo^{IV}, Mo^V, and Mo^{VI} states of chicken liver SO suggested that chloride was coordinated to Mo^{IV} and Mo^V at low pH and high chloride concentration.[49] However, more recent EXAFS experiments using human SO could not completely duplicate the earlier EXAFS results on chicken SO.[50] Indeed, the analysis of the low pH/high chloride Mo^V data for human SO suggests three Mo−S bonds[50] which is in agreement with the present work. Clearly, the EXAFS spectroscopy of chicken liver SO needs to be repeated in view of the discrepancies with the EXAFS data for human SO[50] and our ESEEM and kinetic data[10] on chicken liver SO.

Conclusions

A combination of ESEEM experiments were used to definitively show that Mo^V in the *hpH* form of SO coordinates a group that includes one solvent-exchangeable D(H), probably in the form of a Mo−OH(D) moiety. The orientation of this group is not fixed (although it is substantially restricted) and thus gives rise to a distribution of *hfi* parameters. The resulting loss of amplitude makes direct observation of a proton-related line using ESEEM impossible; however, such a line is observable in ESEEM spectra of the comparable deuterated enzyme.

Numerous ESEEM experiments with the *lpH* form of SO, in H_2O and D_2O buffers, failed to show evidence for any nearby nucleon other than the exchangeable proton/deuteron previously detected by CW EPR. Extensive simulations revealed a small set of geometries in which a nearby H(D) could be present but undetectable; however, these geometries call for unusually long O−H bond lengths and essentially trigonal planar bonding about the oxygen atom. It is considered more likely that in both the *lpH* and *hpH* forms of the enzyme the nearby exchangeable proton/deuteron is part of a Mo−OH(D) moiety and that the spectroscopic differences between the two forms result from a relatively small displacement of the H(D) which moves the nucleon in and out of a node of the singly occupied Mo d orbital. Single-crystal ENDOR studies provide precedent for such behavior,[48] and recent kinetic investigations provide a possible mechanistic explanation for why such a displacement might arise.[10] To further test this hypothesis, as well as to explain the unusually small q_o observed in the *hpH* form of SO, we have now initiated detailed quantum chemical calculations and are preparing model compounds to mimic the observed differences between the *lpH* and *hpH* forms.

Acknowledgment. We thank W. A. Wehbi for assistance in the enzyme purification, and Drs. P. Basu and F.A. Walker for helpful discussions. We thank Dr. Graham George and Professor K. V. Rajagopalan for helpful discussions and information about the EXAFS of human SO prior to publication. Financial support received from the National Institute of Health (Grant GM 37773), the National Science Foundation (Grants DIR 9016385 and BIR 9224431 for the EPR spectrometer), and the Materials Characterization Program of the University of Arizona are gratefully acknowledged.

Supporting Information Available: Two-pulse normalized FT ESEEM spectra of the *Pi* form of SO in D_2O at g_x and g_z; comparison of two-pulse normalized FT ESEEM spectra of the *Pi* and *hpH* forms of SO in H_2O at g_x and g_z; FT ESEEM spectra of the *hpH* forms of SO in D_2O, with the matrix deuteron contributions removed, collected at various magnetic field strengths; four-pulse *s*-line shapes of *lpH* SO in D_2O at various magnetic field strengths (8 pages, print/PDF). See any current masthead page for ordering information and Web access instructions.

JA981903J

(49) George, G. N.; Kipke, C. A.; Prince, R. C.; Sunde, R. A.; Enemark, J. H.; Cramer, S. P. *Biochemistry* **1989**, *28*, 5075−5080.

(50) George, G. N.; Garrett, R. M.; Rajagopalan, K. V., unpublished results.